International Journal of Concrete Structures and Materials

RESEARCH

Open Access

# Influence of Fascinating Diatom *Fragilaria* and *Synechocystis* Cyanobacteria on the Permeation Performance, Mechanical Properties, and Self-Healing Abilities of Concrete Under Curing Fresh Water and Seawater

A. Serag Farid[1], Shireen T. M. Yousef[1], Mohamed M. Abdelaziz[1*], G. M. Abd-El Hafez[2], Ali A. E. El-Khateb[3] and Khaled N. M. Elsayed[4*]

**Abstract**

This study investigates the impact of innovative diatom and cyanobacteria strains at varying concentrations on microbe concrete. The study examines the behavior of two separate species of microalgae, specifically diatom (*Fragilaria* sp. CCAP1029) and *Synechocystis* PCC 6803 cyanobacteria, on concrete. The study confirmed that bio-concrete has greater strength than conventional concrete across all concentrations. The specimens containing *Synechocystis* PCC 6803 demonstrated a significant enhancement in compressive strength and splitting tensile strength, with a rise of 21.66% and 10.34%, respectively. Furthermore, utilizing all the introduced microalgae significantly reduced the corrosion rate of non-accelerated samples. Additionally, the analysis (SEM and EDX) revealed the existence of microbiological calcite precipitation within the concrete's pores. The study's findings emphasize the effectiveness of the introduced microorganisms in enhancing and improving the mechanical properties and encourage crack healing in microbial concrete.

**Keywords** Microalgae, Microbial concrete, Self-healing, Corrosion rate, Durability, SEM, EDX

## 1 Introduction

Inevitable microcracks pose significant problems to civil engineers because they can compromise the long-term durability of structures. Microcracks, pores, and connected pores make it easy for harmful substances to penetrate, leading to reinforcement corrosion (Banthia et al., 2005; Huseien et al., 2015; Li et al., 2019; Picandet et al., 2009; Stehlík et al., 2015; Yang et al., 2011). Several methods of manual crack repair can help extend the lifespan of structures. However, insufficient maintenance causes many existing structures to deteriorate before reaching their expected lifespan (Yang et al., 2011), raising concerns about the sustainability of traditional repair practices (Agha, 2024; Awad, 2023).

Journal information: ISSN 1976-0485 / eISSN 2234-1315.

*Correspondence:
Mohamed M. Abdelaziz
mma22@fayoum.edu.eg
Khaled N. M. Elsayed
k.elsayed@science.bsu.edu.eg
[1] Civil Engineering Department, Faculty of Engineering, Fayoum University, Faiyum, Egypt
[2] Chemistry Department, Faculty of Science, Fayoum University, Faiyum, Egypt
[3] Civil Engineering Department, Faculty of Engineering, Assiut University, Asyut, Egypt
[4] Present Address: Botany and Microbiology Department, Faculty of Science, Beni-Suef University, Beni-Suef, Egypt

Despite implementing several technological innovations, such as prefabricated mixing systems and industrialized building systems (IBS), long-standing cracks and related problems persist, requiring the reconstruction or demolition of the structure (Lachimpadi et al., 2012). Corrosion of concrete reinforcement can occur even in small fissures because water and ions can enter the pores and destroy the concrete matrix (Dharmabiksham & Murali, 2022; Dharmabiksham et al., 2023; Rais & Khan, 2021). Thousands of new construction projects are completed every year, so maintenance and rehabilitation prices may rise. Estimates place the annual cost of repairing and rehabilitating concrete structures older than five years at around $68 million (Wiktor & Jonkers, 2016). Addressing these challenges requires innovative, sustainable solutions that enhance concrete durability and reduce long-term maintenance demands (Jahami et al., 2023, 2024).

Concrete with self-healing capabilities is an innovative building material that has the ability to reduce concrete deterioration (Amran et al., 2022; Kaushal & Saeed, 2024; Linda et al., 1832; Zeaiter et al., 2023). The self-healing characteristic refers to the ability to heal. The natural ability of concrete to spontaneously fix cracks is known as autonomous healing, and it has been observed for many years (Farid et al., 2024; Fratzl, 2014; Seifan et al., 2018; Yatish Reddy et al., 2020; Zhang et al., 2021). The concrete's ability to self-heal is dependent on precise air exposure conditions. In moisture-rich situations, the concrete can seal its fissures. Shape memory polymers, biological binders, and microcapsules can all help accelerate and precipitate the calcite process(Wang et al., 2022). These agents are triggered when polymers react with atmospheric carbon dioxide in the presence of moisture. Calcite crystallization occurs when carbon dioxide from the atmosphere dissolves in water and combines with the ionic calcium already present in the concrete. According to the references, this method can only handle cracks up to 100 μm wide (Fratzl, 2014; Neville & Brooks, 1987). The white crystal substance formed on concrete fractures is a result of the interaction between these healing agents and the surrounding environment. This reduces the width of the cracks, demonstrating the potential to self-repair. Therefore, introducing chemical or biological additives is important to promote the regularity of healing for larger fractures in concrete. Researchers researched and demonstrated the efficacy of incorporating bacteria into the concrete matrix to achieve self-healing behavior (Dagade & Thakur, 2020; Jadhav & Deore, 2022; Jonkers et al., 2010; Osman et al., 2021). The interaction between urease-producing bacteria and the concrete material is responsible for its self-healing properties.

Urease bacteria combine with nutrients, urea, and highly alkaline concrete to produce calcium carbonate precipitation. This precipitation gradually fills and seals the cracks (Jongvivatsakul et al., 2019). Calcium carbonate ($CaCO_3$) is a solid in freshwater, marine water, and soil conditions (Castanier et al., 1999; Hammes & Verstraete, 2002). Four factors influence precipitation: calcium ions ($Ca^{2+}$), pH ($pK_2(CO) = 10.3$ at 25 °C), dissolved inorganic carbon (DIC), and nucleation sites. The pH range is 1–9, inclusive.

Multiple carbonate precipitates from various environments have been linked to different microorganisms. Microorganisms increase carbonate precipitation by creating an alkaline environment with a high pH and increasing quantities of dissolved inorganic carbon using physiological mechanisms (Hammes & Verstraete, 2002; Tittelboom et al., 2010). Three different types of microalgae can cause carbonate precipitation: (i) photosynthetic microorganisms like microalgae and cyanobacteria; (ii) nitrogen cycle-specific microorganisms; and (iii) sulfate-reducing bacteria (Bending et al., 2017). Photosynthetic microorganisms, such as microalgae, use urea amidolyase or urease enzymes to metabolize urea and generate biocement via biocementation. Microalgae, often regarded as microscopic organisms with high photosynthetic capabilities, have piqued the interest of academics and environmentalists due to their outstanding adaptability and broad range of potential applications in various disciplines (Ariyanti, 2012). Photosynthetic cyanobacteria are responsible for the majority of aquatic MCIP production (Whiffin, 2004). Photosynthesis uses carbon dioxide ($CO_2$) according to Eq. 1, which is in equilibrium with carbonate ions ($CO_3^{2-}$) and bicarbonate ions ($HCO_3^-$) as described in Eq. 2. Photosynthetic bacteria assimilate $CO_2$, generating a shift in equilibrium and an increase in pH (as indicated by Eq. 3) (Whiffin, 2004). Equation 4 creates calcium carbonate with calcium ions (Hammes & Verstraete, 2002). Due to the insolubility, the deposited calcite minerals refined the pores and improved the characteristics of concrete.

$$CO_2 + H_2O \rightarrow (CH_2O) + O_2 \tag{1}$$

$$2HCO_3^- \leftrightarrow CO_2 + CO_3^{-2} + H_2O \tag{2}$$

$$CO_3^{-2} + H_2O \leftrightarrow HCO_3^- + OH^- \tag{3}$$

$$Ca^{+2} + HCO_3^- + OH^- \leftrightarrow CaCO_3 \downarrow + 2H_2O \tag{4}$$

Heterotrophic organisms have the potential to precipitate calcite ($CaCO_3$). This cyanobacterium produces bicarbonate, or carbonate, and modifies the system to

promote carbonate precipitation (Castanier et al., 1999). Equation 5 depicts the abiotic breakdown of gypsum ($CaSO_4{\cdot}H_2O$), which results in a system with a high concentration of calcium and sulfate ions. When there is organic matter but no oxygen, sulfate-reducing bacteria can convert sulfate to $H_2S$ and $HCO_3^-$, as demonstrated in Eq. 6 (Garg et al., 2023; Hammes & Verstraete, 2002; Khanafari et al., 2011; Whiffin, 2004).

The system's pH rises when hydrogen sulfide ($H_2S$) is emitted from the environment. When the level of supersaturation reaches a certain point, calcium ions in the system induce calcium carbonate to form. Fig. 1 depicts the mechanism of calcium carbonate precipitation induced by the urease enzyme, which explains (A) that Ca ions are attracted to the surface cells. Urea is introduced, releasing dissolved inorganic carbon (DIC) and ammonia (AMM) into the environment. (B) The entire cell is enclosed; (C) The process of calcium carbonate precipitation follows (Castanier et al., 1999; Hammes & Verstraete, 2002). Microalgae are becoming increasingly essential in concrete production (Lam et al., 2024), a pioneering field that combines biotechnology with construction materials research (Nur & Dewi, 2024).

$$CaSO_4 \cdot H_2O \rightarrow Ca^{2+} + SO_4^{2-} + 2H_2O \tag{5}$$

$$2(CH_2O) + SO_4^{2-} \rightarrow HS^- + HCO_3^- + CO_2 + H_2O \tag{6}$$

The presence of calcium carbonate reduces the permeability of concrete, preventing the ingress of aggressive ions such as chloride ($Cl^-$) that accelerate steel reinforcement corrosion (Muynck et al., 2010; Wiktor & Jonkers, 2011). The key reactions that protect the rebar are passive film formation on steel surface and corrosion prevention by carbonate layer. Steel reinforcement in concrete is typically protected by a passive oxide layer ($Fe_2O_3$ or $Fe_3O_4$), which forms in alkaline conditions as illustrated in Eq. 7 (Ramachandran et al., 2001):

$$4Fe + 3O_2 + 6H_2O \rightarrow 4Fe(OH)_3 \tag{7}$$

This passive film is stable at high pH (> 12.5), which is maintained by the microbial activity-induced precipitation of $CaCO_3$ (Jonkers & Schlangen, 2008). The deposition of $CaCO_3$ on the rebar surface forms a protective barrier, preventing further oxidation and reducing corrosion rate as illustrated in Eqs. 8 and 9 (Tittelboom et al., 2010). This reaction helps mitigate the rusting process by reducing the availability of free $Fe^{2+}$ ions needed for corrosion propagation.

$$Fe_2^+ + CO_3^{-2} \rightarrow FeCO_3 \downarrow \tag{8}$$

$$Fe(OH)_3 + CO_3^{-2} \rightarrow FeCO_3 \downarrow + 3OH^- \tag{9}$$

There are inadequate studies investigating the impact of microalgae and cyanobacteria deposition on the corrosion rate of steel reinforcement in reinforced concrete. This study looks into the effects of adding two promised species of microalgae, one each is diatom, and the other is cyanobacteria strain on the corrosion rate of concrete rebar. The accelerated corrosion method measured the rebar corrosion rate during a given period. Furthermore, the study investigates self-healing ability and the compressive and splitting tensile strengths while comparing freshwater and seawater treatments. The form of the

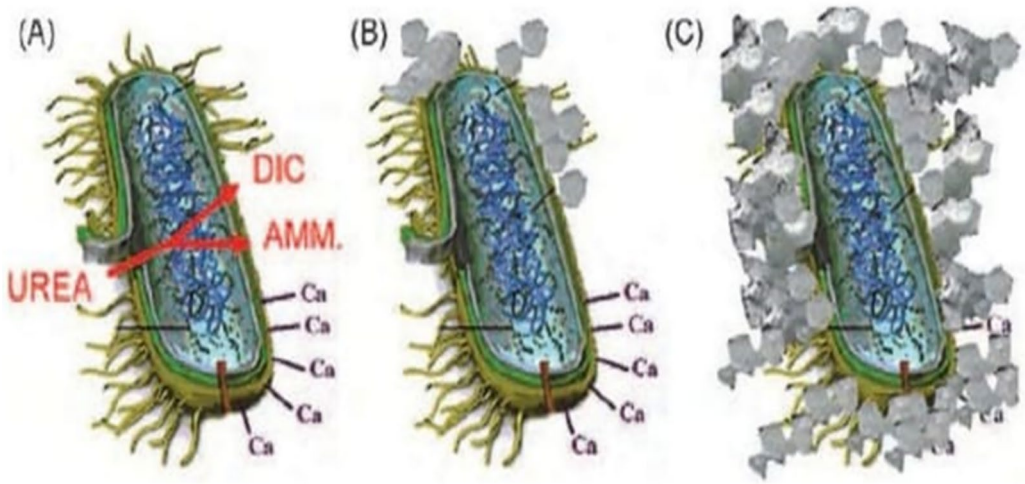


**Fig. 1** An illustration depicting the mechanism of calcium carbonate precipitation generated by the activity of the urease enzyme in microorganisms. (**A**) Ca ions are attracted to the surface cells. Urea is introduced, releasing dissolved carbon (DIC) and ammonia (AMM) into the environment. (**B**) The entire cell is enclosed. (**C**) The process of Calcium Carbonate precipitation follows (Gupta et al., 2013)

sediment in control and cured specimens was further studied using scanning electron microscopy (SEM) and energy-dispersive X-ray spectroscopy (EDX).

## 2 Research Significance

The current study assesses the effects of recently isolated microalgae and cyanobacteria on concrete. The study investigates the behavior of two separate species of microalgae, specifically diatom (*Fragilaria* sp. CCAP1029) and *Synechocystis* sp. PCC 6803 cyanobacteria, on concrete. Different microalgal concentrations are used for each species. An assessment and comparison are made of the microbial concrete's abilities in self-healing, corrosion rate, compressive strength, and splitting tensile strength.

## 3 Materials and Methods

This section describes the materials used in the study, including the preparation and cultivation of microalgae, the mix design, and the experimental procedures for evaluating mechanical properties, durability, and self-healing efficiency.

### 3.1 Materials

The materials used in this study include microalgae (diatoms and cyanobacteria), cement, aggregates, and water. The preparation of microalgae, including their cultivation and growth conditions, is described below.

#### *3.1.1 Enhancement of Algae Cultivation and Growth*

To optimize the effectiveness of microbial concrete, the selected strains of *Fragilaria* sp. CCAP1029 (diatom) and *Synechocystis* sp. PCC 6803 (cyanobacteria) were cultivated under controlled conditions to ensure high biomass production.

*3.1.1.1 Microalgae Cultivation* The cyanobacteria strain *Synechocystis* sp. PCC 6803 was provided by the Botany and Microbiology Department at the Faculty of Science, Beni-Suef University, Egypt, as described by (Elsayed et al., 2017). Subsequently, it was subcultured on Wuxal media, wastewater from FSF, and molasses derived from sugar beet to produce high biomass. The physical and chemical wastewater analysis was conducted at the Tabbin Institute Metallurgical Studies Central Lab for the Studies of Industrial Pollution in Cairo, Egypt. The results are presented in Table 1 and Similarly, the physical and chemical analysis of molasses was carried out at FSF's quality control laboratory.

The relevant data can be found in Table 2. Wuxal media is a marketable fertilizer called Wuxal-Universal dünger. It consists of 8% $P_2O_5$, 8% N, 0.01% B,6% $K_2O$, 0.02% Fe, 0.004% Cu, 0.004% Zn, and 0.012% Mn. This data was supplied by Elsayed et al. (Mohamed et al., 2022). The fertilizer is produced by Wilhelm Haug GmbH & Co. KG in Germany. *Synechocystis* sp. *PCC 6803* was cultivated in 2000-mL Erlenmeyer containers at 30 °C with 12 h of light (30 µmol photons/$m^2$/s) followed by 12 h of darkness. A spectrophotometer with a wavelength of 730 nm was used to establish the growth curves of microalgae on three different media.

**Table 1** The physical and chemical components of the wastewater collected from Fayoum Sugar Factory (Fayoum city, Egypt), used for microalgal cultivation

| Factor | Result | Unit |
|---|---|---|
| Temperature | 26.76 | °C |
| pH 7.56 | 7.57 | – |
| Dissolved oxygen | 6.1 | mg\L |
| COD Cr | 20.3 | ppm |
| BOD (5d, 20 °C) | 10.2 | ppm |
| Total suspended salts | 20.1 | ppm |
| Total dissolved solids | 856 | ppm |
| Total phosphorus | 0.41 | ppm |
| Total nitrogen | 0.542 | ppm |
| Ammonia as $NH_3$ | 0.533 | ppm |

**Table 2** The chemical and physical components of molasses derived from sugar beet Factory (Fayoum city, Egypt) to produce high biomass used for microalgal cultivation

| Factor | Result | Unit |
|---|---|---|
| Protein | 9 | % |
| Sucrose | 49 | % |
| Betaine | 6 | % |
| pH | 7.5 | – |
| Density | 1400 | Kg/$m^3$ |
| Ash | 10 | % |
| Water | 20 | **%** |

*3.1.1.2 Isolation and Cultivation of Microalgae Strains* This investigation identified one distinct strain of microalgae. The diatom strain *Fragilaria* sp. CCAP1029 was evaluated using several microbiological parameters. Precisely, both the isolated strains of *Fragilaria* sp. CCAP1029 and *Synechocystis* sp. PCC 6803 examined under the phase contrast microscope at magnification of objective lens 40X and ocular lens of 20X with total magnification power 800X (light microscope in Fig. 3 (Carl ZEISS Primo Star Light Microscope, Japan) and morphological observations done such as shape, color, cellular form and structure also compared with standard identified samples according to Dev et al. (2025), Verma and Kaur (2020).

Firstly, visualization was used to isolate and refine various microalgal strains from water and soil samples. (1) Collected water and soil samples from specific areas in Egypt specially Beni-Suef area with a 50-mL Falcon tube. The selecting criteria for isolation of these strains based on (a) choosing mid-way area between Egypt north and south at which the temperature and light intensity are moderate and very suitable for growing microalgae during different seasons of the year (Beni-Suef city), (b) In economical point of view, we focused on domestic growing strains under normal outdoor conditions, and (c) Easy to isolate and cultivate. (2) The water samples were centrifuged at 3500 rpm for 10 min. (3) The liquid portion above the sediment was removed. (4) Resuspend the pellets with the remaining liquid. (5) With a wire loop, the 13-streak approach was used to pick the cyanobacteria onto a BG11 agar plate. (6) The plates were incubated at 30 °C under continuous light (30 µmol photons/$m^2$/s) until reaching the highest exponential growth phase which commonly takes place between 10 to 14 days in most published data (Joseph et al., 2014). (7) To improve growth, transfer individual green colonies from a mixed culture to a fresh BG11 agar plate using the 13-streak method and incubate as described in step (6). Carefully, both the pure uni-algal isolated strains *Synechocystis* sp. PCC 6803 and *Fragilaria* sp. CCAP1029 transferred from Bg11 agar plates to sterilized cultivation flasks of 2 L, and finally bottles of 25 L with continuous aeration at 30 °C under continuous light (30 µmol photons/$m^2$/s) and controlled every two days by counting the cells number/ml using hemocytometer (counting chamber) with the following formula to get final concentrations $10^3$, $10^5$ and $10^7$ cells /ml.

$$\text{Cells/mL} = (\text{Cell count})/(\text{number of chambers counted}) \times \text{dilution} \times 10^4$$

(Nur & Dewi, 2024) as illustrated in Figs. 2, 3 (Delgado et al., 2015).

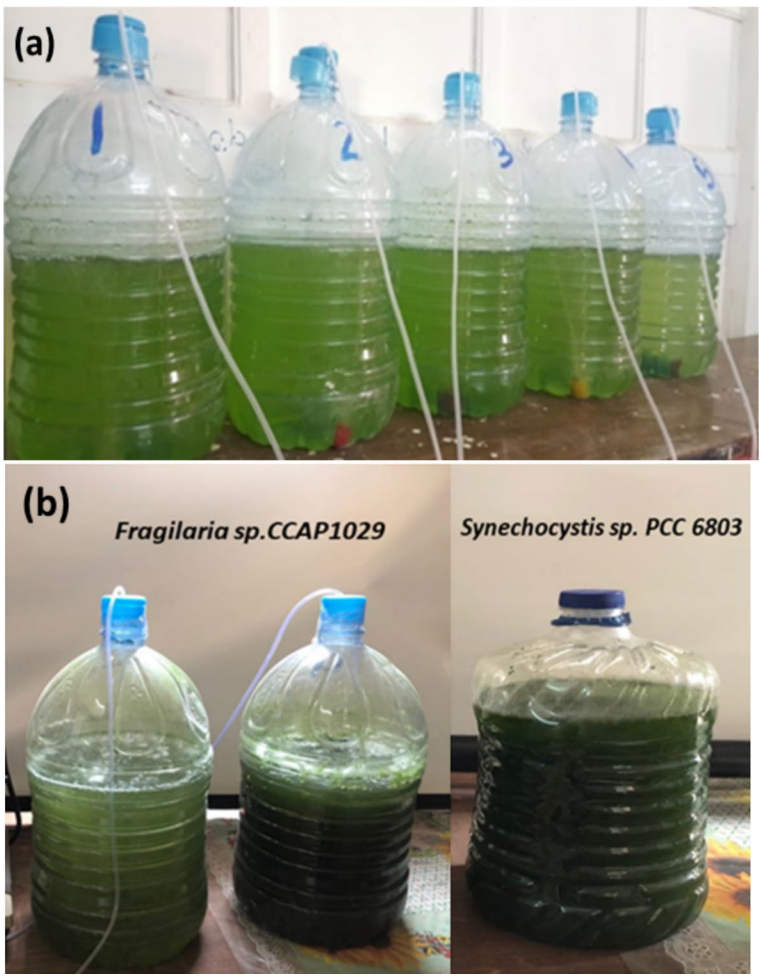


**Fig. 2** **a** Cultivation of isolated microalgae strains under continuous aeration at 30 °C under continuous light (30 µmol photons/$m^2$/s). **b** Microalgae solutions with different concentrations

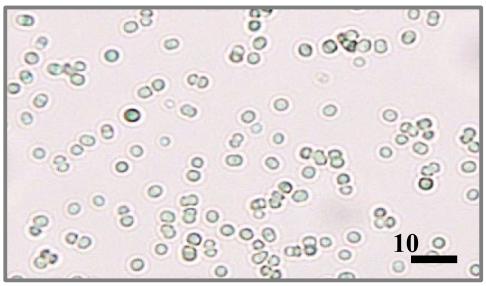


*Synechocystis sp.* **PCC 6803**

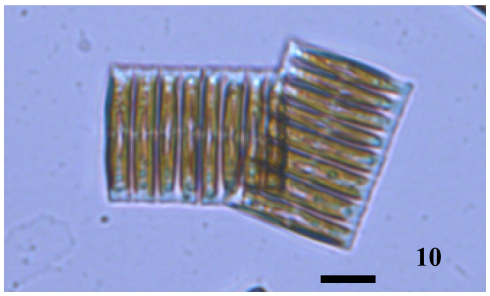


*Fragilaria sp.* **CCAP1029**

**Fig. 3** Microscopic view showing the isolated diatom and cyanobacterium strains (total magnification of 800X, light microscope (Carl ZEISS Primo Star Light Microscope, Japan)

**Table 3** The particle size distribution of crushed dolomite and sand

| Sieve size(ASTM) | | Total (%) Retained cumulative | Total (%) Passing |
|---|---|---|---|
| standard | Alternate | | |
| Coarse sieves (crushed dolomite) | | | |
| 37.5 mm | 1.5in | – | 100 |
| 25 mm | 1in | – | 100 |
| 19 mm | 3/4in | – | 100 |
| 12.5 mm | 1/2in | 13.89 | 86.11 |
| 9.5 mm | 3/8in | 84.77 | 15.23 |
| 4.75 mm | No.4 | 98.9 | 1.1 |
| Fine sieves (sand) | | | |
| 4.75 mm | No.4 | – | 100 |
| 2.37 mm | No.8 | 1.7 | 98.3 |
| 1.18 mm | No.16 | 11.2 | 88.8 |
| 600 µm* | No.30 | 33.1 | 66.9 |
| 300 µm | No.50 | 81.65 | 18.35 |
| 150 µm | No.100 | 97.2 | 2.8 |

* 1000 µ(micro-meter) = 1mm

**Table 4** Physical characteristics of crushed dolomite and sand

| Property | Volume weight (t/m$^3$) | Fineness modulus | Specific gravity (t/m$^3$) | Absorption rate (%) |
|---|---|---|---|---|
| Crushed dolomite | 2.52 | 2.24 | 1.49 | 1 |
| Natural sand | 2.51 | 2.43 | 1.71 | 0.91 |

#### *3.1.2 Aggregates*

Fine and coarse aggregates of sand and crushed dolomite were utilized. The grading of the aggregates was determined through sieve analysis, as depicted in Table 3. Furthermore, Table 4 displays the specific characteristics of the aggregates. The examination findings adhere to the requirements given in BS EN 12620:2002 (2008) (S. Recommendation, 2016).

**Table 5** Mechanical characteristics of ordinary Portland cement (OPC)

| Properties | Limitation | Result |
|---|---|---|
| Fineness | Not less than 2750 cm$^2$/gm | 4232 cm$^2$/gm |
| Initial setting time | Not less than 45 min | 75 min |
| Final setting time | Not more than 10 h | 200 min |
| Compression strength after 3 days | Not less than 180 kg/cm$^2$ | 268 kg/cm$^2$ |
| Compression strength after 7 days | Not less than 270 kg/cm$^2$ | 365 kg/cm$^2$ |
| Expansion | Not more than 10 mm | 1.5 mm |

#### *3.1.3 Cement*

This study utilized ordinary Portland cement of grade 42.5, which meets the requirements of ASTM C-150 Type I standards (Cement & Apparatus, 2016). Table 5 summarizes the cement's qualities based on experimental testing.

#### *3.1.4 Water*

The water utilized during the casting process was fresh and free of contaminants, acids, oils, salts, and organic molecules. The freshwater is pure and meets the standards defined by ASTM D 1193 (Method, 2018). The specimens were treated with both fresh water and seawater. Table 6 shows the chemical analysis of Fayoum's seawater supplied from Lake Qarun.

#### *3.1.5 Mixture Design*

The control mixture for this study was constructed according to the criteria stated in ACI 318-19 (I. Units, An ACI Standard). A water-to-cement ratio (w/c) of 0.45 was employed to attain the target compressive strength of 30 MPa in 28 days. The distribution of the various blends is shown in Table 2. The control mixture had compressive strengths of 21.57 MPa, 30.9 MPa, and 39.70 MPa

**Table 6** The chemical analysis of seawater (Qaroun Lake)

| Property | Result |
|---|---|
| Density | 1.035 gm/cm$^3$ |
| Sulfate | 9.722 gm/l |
| Chlorides | 12.975 gm/l |
| Sodium | 10.097 gm/l |
| Magnesium | 1.335 gm/l |
| Bicarbonate | 0.315 gm/l |
| Calcium | 0.550 gm/l |
| Carbonates | 0.034 gm/l |
| Others | 0.474 gm/l |
| Ions | – |

after 7, 28, and 90 days, respectively. A study determined the effect of microalgae (*Fragilaria* sp. *CCAP1029*) and cyanobacteria (*Synechocystis* sp. *PCC 6803*) on concrete. The study assessed the different concentrations of each vegetative microorganism. In addition, the study looked at mechanical qualities, durability, permeability (corrosion rate), and self-healing efficiency. Table 7 shows the ingredient quantities used in the mix design.

Compressive and splitting tensile strength tests were performed on specimens using 100 mm cubes and 100 mm × 200 mm cylinders, respectively. The tests were carried out with a compression test device at 7, 28, and 90-day intervals, following the directions provided in IS 516+2021.

### 3.2 Experimental Tests

#### *3.2.1 Compressive and Splitting Tensile Strengths*

The compressive and splitting tensile strengths were measured using 100 mm cubes and cylindrical specimens with 100 mm diameter and 200 mm length, respectively. The concrete mixture was precisely poured into cubes and cylinders, which were then compacted using a vibrating table, as shown in Fig. 4a. As per ASTM C 192 (Mohamed et al., 2022), all specimens were retrieved from the molds after 24 h and then immersed in a water medium, which might be freshwater or seawater, as shown in Fig. 4b. Specimens were obtained from the processed water 24 h before the experiment.

#### *3.2.2 Corrosion Rate*

Concrete permeability was tested using cylindrical specimens with diameters of 70 mm and lengths of 100 mm. Concrete was carefully poured into cylinders, which were then vibrated. After one day, all specimens were removed from the molds and cured for 28 days in fresh or seawater before being tested for corrosion rate. Reinforced cylinders were immersed in freshwater, seawater, or saline reference solutions for 24 h. Thoroughly soaked specimens provide accurate corrosion results. During corrosion rate testing on reinforced cylindrical specimens, anode electrons encountered water and oxygen, generating hydroxyl ions at the cathode. Electricity was transmitted using steel rods. Oxygen and water produce hydroxyl and ions, leading to the corrosion of reinforcing steel. The corrosion was assessed, and the reinforced cylinders were extracted from the processing water. They were maintained in a dry state for one day. The procedure was conducted in a plastic tank filled with fresh water, seawater, and 5% sodium chloride (Kanwal et al., 2023). A Stainless steel plate and bar were connected to the power supply's negative and positive terminals respectively. Establishing a parallel connection of the reinforced cylindrical samples formed an electrochemical circuit for the cathode plate.

A potentiometer controlled the circuit's current for dependable testing, while a multimeter maintained the correct amperage. When an iron atom loses two electrons at the anode, the electrolyte absorbs a positive iron ion ($Fe^{+2}$) (Eq. (10)). Free electrons mix with electrolyte components to make hydroxide ions ($OH^-$), which then react with ferrous ions to form ferric hydroxide (Eq. (11)).

The imposed current hastens ferric hydroxide oxidation-induced black rust deterioration. The stainless

**Table 7** Mix design

| Mixture | Cement Kg/m$^3$ | Sand Kg/m$^3$ | Dolomite Kg/m$^3$ | Freshwater Kg/m$^3$ | Algae (cell/ml $_{water}$) | Description |
|---|---|---|---|---|---|---|
| cs | 435.15 | 810.34 | 956.67 | 194.15 | – | Control |
| FS-C1 | 435.15 | 810.34 | 956.67 | 194.15 | $10^5$ | *Fragilaria* sp.*CCAP1029* |
| FS-C2 | 435.15 | 810.34 | 956.67 | 194.15 | $10^7$ | |
| FS-C3 | 435.15 | 810.34 | 956.67 | 194.15 | $10^9$ | |
| SSS-C1 | 435.15 | 810.34 | 956.67 | 194.15 | $10^3$ | *Synechocystis* sp. *PCC 6803* |
| SSS-C2 | 435.15 | 810.34 | 956.67 | 194.15 | $10^4$ | |
| SSS-C3 | 435.15 | 810.34 | 956.67 | 194.15 | $10^5$ | |

(a)

(b)

**Fig. 4** Preparation steps: **a** casting and filling cubes and cylinders; **b** curing specimens in both freshwater and seawater

steel cathode decreases oxygen by consuming electrons from iron oxidation; Eq. (12) results from air oxygen molecules. Increased rust breaks down concrete. After operations were halted, corrosion-ridden cylinders were inspected.

$$Fe \rightarrow Fe^{+2} + 2e^{-} \tag{10}$$

$$Fe^{+2} + 2\,OH^{-} \rightarrow Fe(OH)_2 \tag{11}$$

$$Fe(OH)_2 + O_2 + 2H_2O \rightarrow 4Fe(OH)_3 \tag{12}$$

LPR (Linear Polarization Resistance) was used to assess corrosion. This corrosion rate test is popular due to its adjustability and non-destructive nature. Steel bar potential is constantly changed and compared to an open circuit. A computer-linked measurement system employs VOLTAMASTER 4 software as a corrosion tank, with the concrete specimen serving as the working electrode, a reference electrode, and a counter-electrode to collect data. The breaking of the protective coating on steel reinforcement causes concrete corrosion. Chloride ions cause this rupture, carbonation, and repeated freezing and thawing (Yuvaraj et al., 2022). Testing is faster, and steel corrosion increases with induced current. Anodizing the concrete specimen promotes the corrosion of steel bars. Thus, a 12-V DC provided the electrochemical circuit with a 1 mA/cm$^2$ current density.

#### *3.2.3 Self-Healing Efficiency*

Experiments on 100 mm × 100 mm × 500 mm beam specimens with a 12 mm rebar in the middle assessed self-healing efficiency. The beams were cured for 28 days in either fresh or seawater. After the water was removed, the beams were allowed to dry for 24 h. The hydraulic compression machine's loading surfaces were suitably spaced to provide consistent support and loading point distances. The loading direction corresponded to the response direction, as vertical weight was applied until cracks developed. Two crack-healing fluids were employed to repair beam cracks. The control beams were treated with a microbiological solution, whereas the algal beams were treated with both fresh water and seawater.

**Table 8** Details of the healing treatment

| Category | Type of algae application | Healing status |
|---|---|---|
| CS-1 | External | A solution of Diatom(*Fragilaria*) |
| CS-2 | External | A solution of *Synechocystis* sp. |
| FS-A | Internal ($10^5$ Diatoms(*Fragilaria*)cells/ml) | Fresh-water |
| SSS-B | Internal ($10^3$ *Synechocystis* sp. cells/ml) | Fresh-water |
| FS-a | Internal ($10^5$ Diatoms(*Fragilaria*) cells/ml) | Sea-water |
| SSS-b | Internal ($10^3$ *Synechocystis* sp. cells/ml) | Sea-water |

Table 8 summarizes specimens, microbial treatment, and healing.

#### *3.2.4 Microstructural Characteristics*

*3.2.4.1 Scanning Electron Microscope (SEM) and Energy Dispersive X-ray Spectroscopy (EDX) Mapping* Scanning Electron Microscopy (SEM) is a valuable scientific tool for thoroughly examining and analyzing a specimen's shape, structure, and substance at the microscopic level. A detailed microscopic analysis using meticulously chosen fragmented chips from the examined samples. Gold was carefully applied to the chips as a protective covering to address the issue of electron charging on the concrete molecules. This decision was taken because gold has conductive properties, effectively reducing charging effects. Flat and small chips were chosen to provide the finest possible image quality, contrast, and brightness. This decision also sought to decrease the possibility of surface wrinkling, which might lead to charge accumulation. The fragments were examined by SEM, after which they were subjected to EDX analysis.

## 4 Results Analysis and Discussion

### 4.1 Compressive Strength Test

The compressive strength of the specimens was measured at three time points: 7, 28, and 90 days after treatment in freshwater and seawater. For each sample, three cubes were tested for compressive strength. The average values were used for comparison across different samples to ensure consistency and reliability. Table 9 compares the compressive behavior of diatom (*Fragilaria* sp. *CCAP1029* specimens) (FS-C1, FS-C2, and FS-C3) and *Synechocystis* sp. *pcc6803* (SSS-C1, SSS-C2, and SSS-C3) mixes to that of the control specimen mix. The control specimen mix was utilized to test strengths at various curing intervals. Concrete samples with different algae showed increased compressive strength compared to the control. Calcite precipitates through algae-filled matrix fissures. It has been demonstrated that both algal concentrations tested resulted in increased strength across all ages. Two mechanisms increase compressive strength. Alga-derived β-carotene pigment fills concrete holes by increasing electron density. Despite its regular green appearance, the alga's orange color is caused primarily by naturally occurring pigments such as carotenoids or droplets. Another aspect is algal metabolic activity, which includes the creation of calcite minerals (Taher et al., 2020). The study discovered that the algae cubes in the *Synechocystis* sp. pcc6803 (SSS-C1) sample, the optimal mix, showed a greater increase in their strengths than the other samples.

After 28 days, the cubes were treated with freshwater at $10^5$ cells/ml concentration for *Fragilaria* sp.*CCAP1029* and $10^3$ cells/ml for *Synechocystis* sp. *pcc6803,* which demonstrated the best compressive strength. Table 9 shows the percentage increase in compressive strength after algae introduction. The results showed a significant increase in compressive strength: 22.33% after introducing *Fragilaria* sp. *CCAP1029* at $10^5$ cells/ml concentration and 18.12% after adding *Synechocystis* sp.*pcc6803* at $10^3$ cells/ml. Furthermore, after 7 days of curing with algal components in fresh water, the compressive strengths of the concrete specimens exceeded those of the control specimen during the same period. This finding is consistent with the findings of Niveditha et al. (2018), who concluded that the efficiency of microorganisms in concrete is mostly determined by the time they offer. Based on the MIP study, the researchers determined that the width of concrete pores increased during the early curing stages. The solution's microalgae-induced calcium carbonate precipitation followed the same mineralization mechanism (Natsi & Koutsoukos, 2022). Nonetheless, partial hydration reduces the size of the cement's pores. The diversity in hole size allows algal cells to readily fit in, resulting in a favorable environment for spore production and calcite mineral accumulation.

The control mix cured with seawater (CS) had compressive strengths of 22.0, 31.3, and 36.3 MPa, respectively. Seawater improved hydration, reduced cement setting time, and boosted concrete's initial strength compared to fresh water. However, this reduced the subsequent strength of the concrete. Chloride ions in saltwater increased calcium hydroxide production at an earlier stage (Gonen & Yazicioglu, 2007; Sikora et al., 2020). This

**Table 9** Comparison of the compressive strengths for algal mixes

| Mixture | a) Freshwater treatment series | | | | | b) SeaWater treatment series | | | | |
|---|---|---|---|---|---|---|---|---|---|---|
| | 7 days | 28 days | 90 days | ±(%) | | 7 days | 28 days | 90 days | ±(%) | |
| | | | | 28 days | 90 days | | | | 28 days | 90 days |
| CS | 21.57 | 30.90 | 39.70 | 0.00 | 0.00 | 22.00 | 31.30 | 36.30 | 0.00 | 0.00 |
| FS-C1 | 26.60 | 37.80 | 41.60 | 22.33 | 5.04 | 24.60 | 36.30 | 40.10 | 15.97 | 9.86 |
| FS-C2 | 23.50 | 35.60 | 40.55 | 15.21 | 2.14 | 22.70 | 32.40 | 39.00 | 3.50 | 6.85 |
| FS-C3 | 22.30 | 35.00 | 39.80 | 13.27 | 0.25 | 21.40 | 32.90 | 37.50 | 5.11 | 2.74 |
| SSS-C1 | 26.20 | 36.50 | 48.30 | 18.12 | 21.66 | 22.30 | 33.30 | 45.10 | 6.39 | 23.56 |
| SSS-C2 | 25.40 | 33.90 | 44.70 | 0 | 12.59 | 26.50 | 34.60 | 40.20 | 1.05 | 10.14 |
| SSS-C3 | 22.00 | 31.80 | 42.50 | 2.91 | 7.05 | 21.90 | 31.00 | 41.30 | −0.96* | 13.15 |

* The (−) sign indicates a decrease in the percentage change

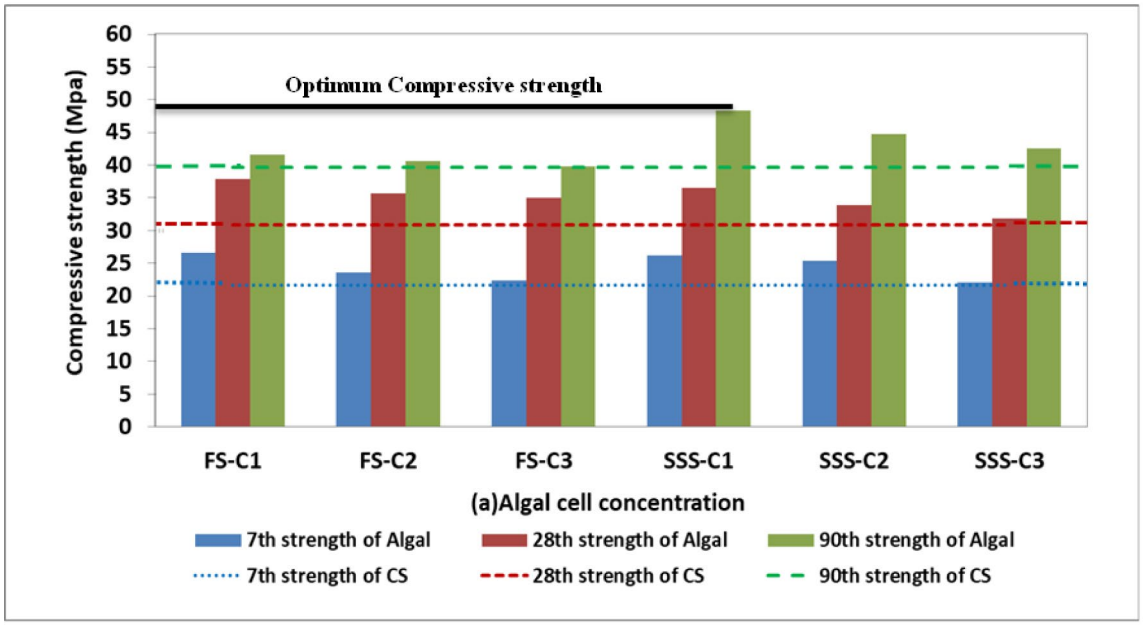


**(a) Compressive strengths under fresh water.**

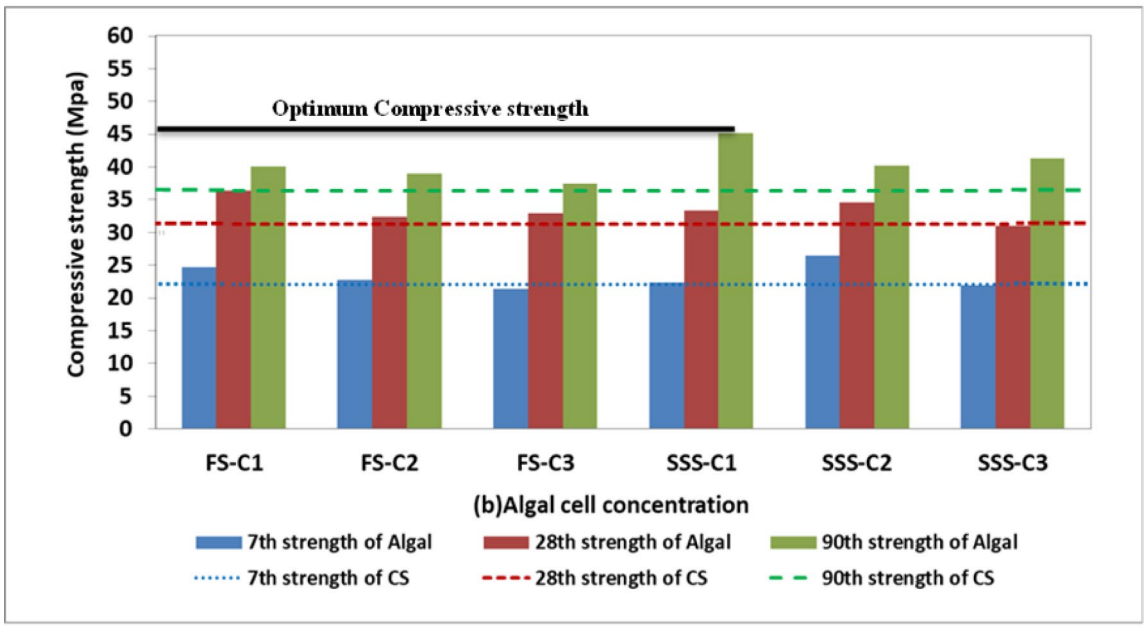


**(b) Compressive strengths under sea water.**

**Fig. 5** Comparison between the compressive strengths of the algal mixes cured with fresh and seawater

study used a seawater-treated CS mix to explore algae's effect on compressive strength under seawater circumstances. Fig. 5b shows that the algae cubes treated in seawater for 90 days had the highest compressive strength at a concentration of $10^3$ cells/ml for *Synechocystis* PCC 6803 and $10^5$ cells/ml for *Fragilaria* sp. CCAP1029. The data indicate that both concentrations of algae tested led to increased strength in all age groups.

**Table 10** Comparison of the splitting tensile strengths for algal mixes

| Mixture | a) Freshwater treatment series | | | | | b) Seawater treatment series | | | | |
|---|---|---|---|---|---|---|---|---|---|---|
| | 7 days | 28 days | 90 days | ± (%) | | 7 days | 28 days | 90 days | ± (%) | |
| | | | | 28 days | 90 days | | | | 28 days | 90 days |
| CS | 2.3 | 2.9 | 3.2 | 0.00 | 0.00 | 2.5 | 3.1 | 3.0 | 0.00 | 0.00 |
| FS-C1 | 2.5 | 3.2 | 3.3 | 10.34 | 3.13 | 2.6 | 3.4 | 3.5 | 9.68 | 16.67 |
| FS-C2 | 2.4 | 3.2 | 3.4 | 10.34 | 6.25 | 2.5 | 3.0 | 3.3 | −3.23* | 10.00 |
| FS-C3 | 2.4 | 3.1 | 3.2 | 6.70 | 0.00 | 2.3 | 3.0 | 3.1 | −3.23* | 3.33 |
| SSS-C1 | 2.1 | 3.2 | 3.45 | 10.34 | 7.81 | 2.5 | 3.2 | 3.5 | 3.23 | 16.67 |
| SSS-C2 | 2.45 | 3.1 | 3.3 | 6.70 | 3.13 | 2.6 | 3.2 | 3.4 | 3.23 | 13.33 |
| SSS-C3 | 2.1 | 3.1 | 3.2 | 6.70 | 0.00 | 2.4 | 3.0 | 3.1 | −3.23* | 3.33 |

* The (−) sign indicates a decrease in in percentage change

### 4.2 Splitting Tensile Strength Test

A total of 63 cylindrical specimens measuring 200 mm in height and 100 mm in diameter were constructed and subjected to a water-curing method for three different periods: 7, 28, and 90 days. This method was carried out in both freshwater and ocean. These specimens were then evaluated for splitting tensile strength using compression testing equipment in accordance with the IS: 516-1959 (1959) specifications. The test results for the control and algal concrete are shown in Table 10.

Fig. 8a shows that the concrete samples containing *Synechocystis* sp.*pcc6803* and *Fragilaria* sp.*CCAP1029* mixes had higher tensile strength than the control samples at 7, 28, and 90 days. However, the rise in compressive strength outpaced the increase in tensile strength. The increased tensile strength observed with microbial concrete may be attributed to the deposition of calcite layers on the concrete surface, with cyanobacteria successfully filling the pores (Dianti, 2017). The results indicate that the optimal concentration of algal cells to achieve a 90-day splitting tensile strength in freshwater was $10^3$ cells/ml for *Synechocystis* sp.*pcc6803* (SSS-C1), resulting in a 7.81% increase, and $10^7$ cells/ml for *Fragilaria* sp.*CCAP1029* (FS-C2), resulting in a 6.25% increase.

The splitting tensile strength of the seawater-cured CS mix was measured to be 2.5, 3.1, and 3.0 MPa at 7, 28, and 90 days, respectively. Compared to freshwater curing, seawater accelerated the reduction in cement setting time and hydration, resulting in a higher early strength of the concrete. Nonetheless, the seawater had a negative impact on subsequent strength, particularly compressive strength. In this study, the saltwater-cured CS mix was used as a benchmark to explore the effect of algae on splitting tensile strength in seawater conditions, as shown in Fig. 6b. The results showed that the most efficient microbe density for achieving a 90-day splitting tensile strength in saltwater was $10^5$ cells/ml of *Fragilaria* sp.*CCAP1029* (FS-C1), resulting in a significant 16.67% increase. The ideal concentration for *Synechocystis* sp.*pcc6803* (SSS-C1) was $10^3$ cells/ml, a 23.3% growth increase.

### 4.3 *Corrosion Rate Study Performed Before Applying an Acceleration (0 mA/cm$^2$)*

Table 11 displays the Linear Polarization Resistance (LPR) test data. A comparison of the corrosion currents of the control mix treated with fresh water and the mix cured with seawater revealed that the latter had approximately 2.5 times the corrosion current. The presence of seawater accelerates the process of cement hydration during the earliest phases, increasing the density and strength of the concrete. Chlorides react with calcium hydroxide (CH), which is generated during cement hydration, to produce calcium chloride ($CaCl_2$) (Li et al., 2021). Choosing the best electrolyte media for both the anodic and cathodic sections of rebar significantly impact how quickly corrosion accelerates. This has been investigated by Dasar et al. (Dasar et al., 2020).

Fig. 7a shows that increasing the quantity of algae cells reduces the maximal anodic currents while improving the passive layer. Microbiological concrete improves impermeability by filling pores with calcites, which increases corrosion resistance (Achal et al., 2011). In general, algal specimens had higher polarization resistance than controls. The specimens produced from *Synechocystis* sp. pcc6803 demonstrated higher durability. For example, the SSS-C1 specimen had a Rp value of 1610 ($\Omega$ cm$^2$), while the CS specimen had a value of 619.76. The sample containing *Fragilaria* sp. *CCAP1029* had a Rp value of 1090 ($\Omega$/cm$^2$). The higher resistivity is due to a larger matrix and the trapping of calcite by algae (Dianti, 2017). Microalgae precipitation influenced the corrosion rate, as treated samples had a higher reduction in corrosion current than control samples. The presence of calcite in the samples reduced corrosion. The study discovered that algal mineral precipitation formed a protective barrier for the passive layer of rebar, preventing corrosion. These findings are consistent with those of Olivia et al. (Olivia et al., 2013).

Fig. 7b shows that the seawater-cured specimens corroded at 1306 mm/year, whereas the freshwater-cured specimens corroded at 430.8 mm/year. Under identical curing circumstances, organisms display decreased corrosion, with algal corrosion happening slower than control corrosion. Chloride ions with a negative charge damage the stable layer of rebar, resulting in corrosion. Corrosion occurs when sufficient chloride comes into contact with the rebar. The continuous creation of chloride ions from the hydrolysis of corrosion products is a critical issue (Osman et al., 2021). Compared to the control group, algae-containing specimens displayed a higher lifespan. Table 11 shows that the introduction of *Synechocystis* sp. *pcc6803* and *Fragilaria* sp. *CCAP1029* microalgae resulted in Rp values of 1190 and 763.70 $\Omega$ cm$^2$, respectively. Seawater treatment has a higher corrosion rate than freshwater treatment.

Furthermore, the current study, represented in Fig. 7c, is the third to investigate the effects of increased salt concentrations on microorganisms. Algal corrosion diminishes when the percentage of sodium chloride increases compared to the control. The intrusion of chlorides into concrete causes material degradation and reinforcement corrosion. Microorganisms that inhibit chloride ion permeability can boost concrete durability and material properties. Algae can infiltrate chloride ions into

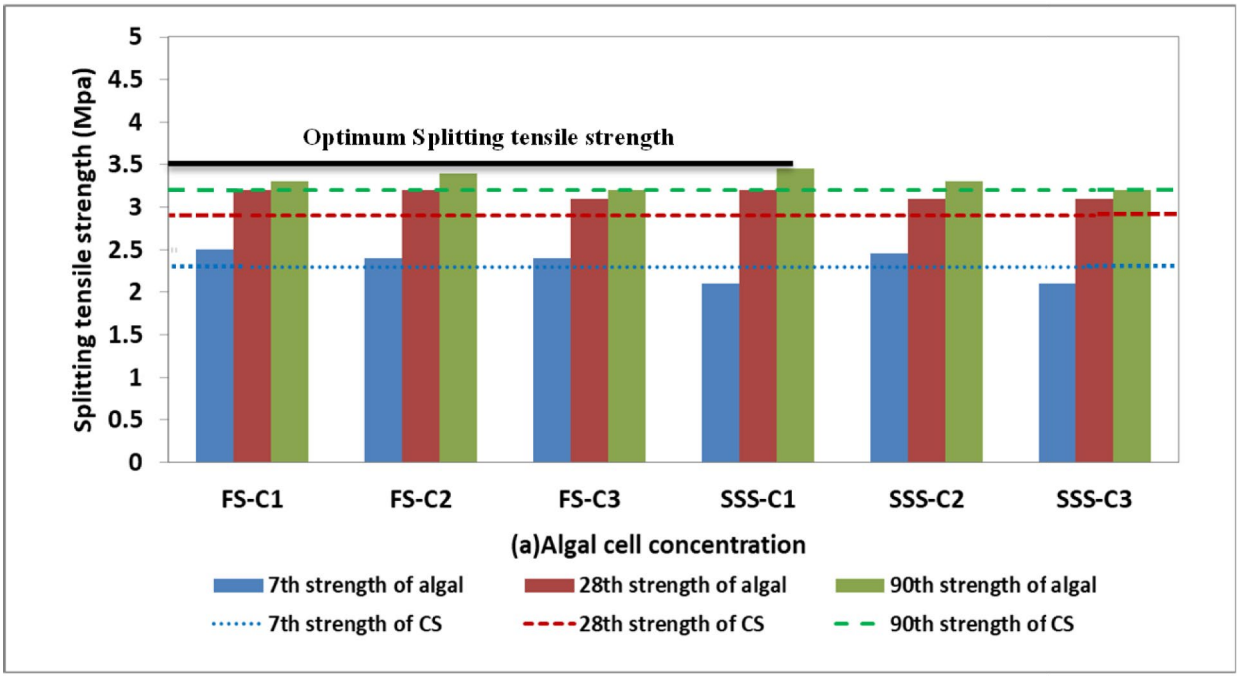


**(a) Splitting tensile strengths under fresh water.**

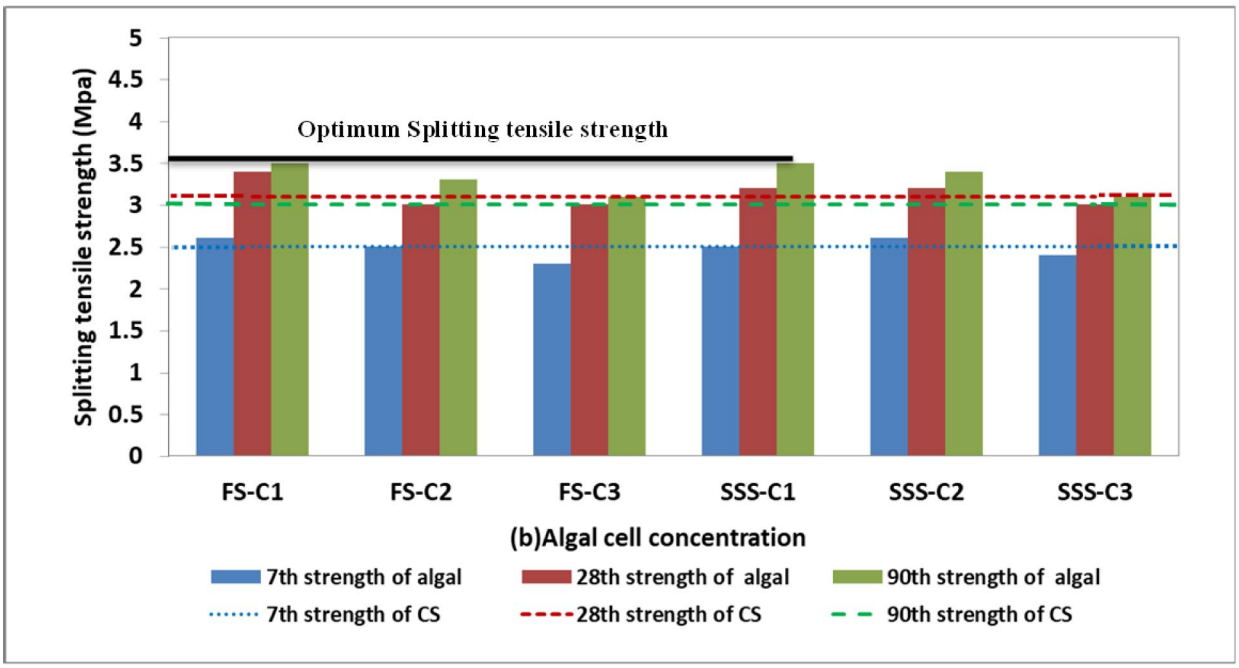


**(b) Splitting tensile strengths under seawater.**

**Fig. 6** Comparison between the splitting tensile strengths of the algal mixes cured with fresh and sea-water

**Table 11** The corrosion investigation data for freshwater, seawater, and saline solution cured series before acceleration (0 mA/cm$^2$)

| Mixture | a) Freshwater treatment series | | | | b) Seawater treatment series | | | | c) Saline solution treatment series | | | |
|---|---|---|---|---|---|---|---|---|---|---|---|---|
| | $E_{corr}$ (mV) | $R_p$ (Ω.cm$^2$) | $I_{corr}$ (μA/cm$^2$) | Corrosion rate (mm/year) | $E_{corr}$ (mV) | $R_p$ (Ω.cm$^2$) | $I_{corr}$ (μA/cm$^2$) | Corrosion rate (mm/year) | $E_{corr}$ (mV) | $R_p$ (Ω.cm$^2$) | $I_{corr}$ (μA/cm$^2$) | Corrosion rate (mm/year) |
| CS | −597.50 | 619.78 | 37.12 | 430.80 | −659.70 | 234.62 | 112.51 | 1306 | −718.60 | 223.87 | 117.70 | 1367 |
| FS-C1 | −569.70 | 1090 | 25.12 | 290.60 | −546.80 | 557.20 | 47.13 | 547.00 | −646.50 | 520.55 | 51.18 | 594.00 |
| FS-C2 | −590.00 | 758.72 | 34.47 | 400.10 | −533.80 | 763.70 | 34.60 | 401.60 | −668.9 | 399.42 | 66.33 | 769.90 |
| SSS-C1 | −478.30 | 1610 | 14.97 | 173.70 | −558.60 | 565.80 | 47.32 | 548.10 | −575.40 | 607.06 | 43.33 | 502.90 |
| SSS-C2 | −486.80 | 1260 | 21.14 | 245.30 | −532.00 | 1190 | 22.38 | 259.80 | −536.00 | 847.17 | 32.22 | 373.90 |

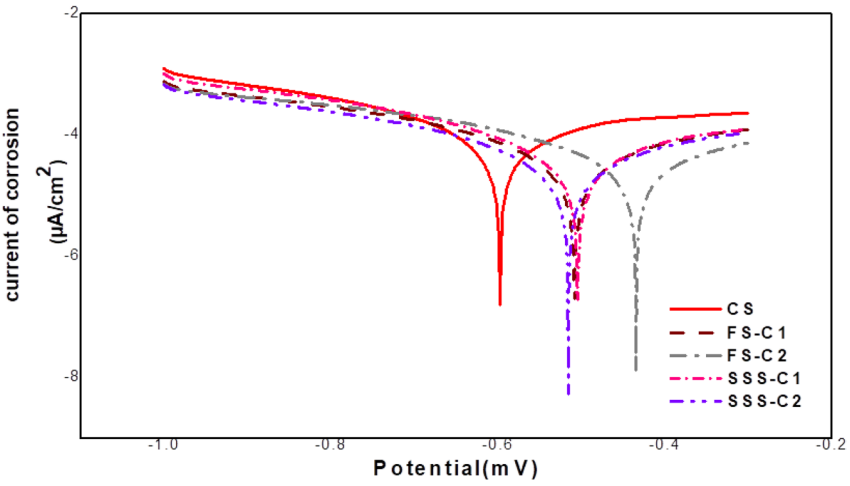


(a)

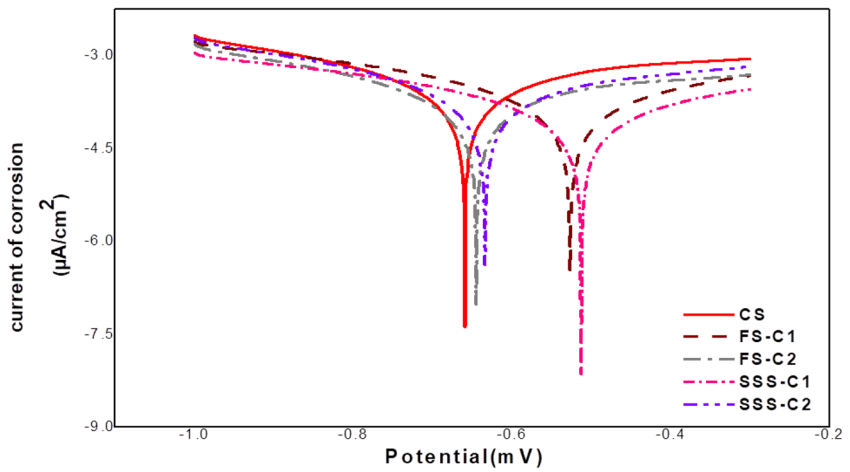


(b)

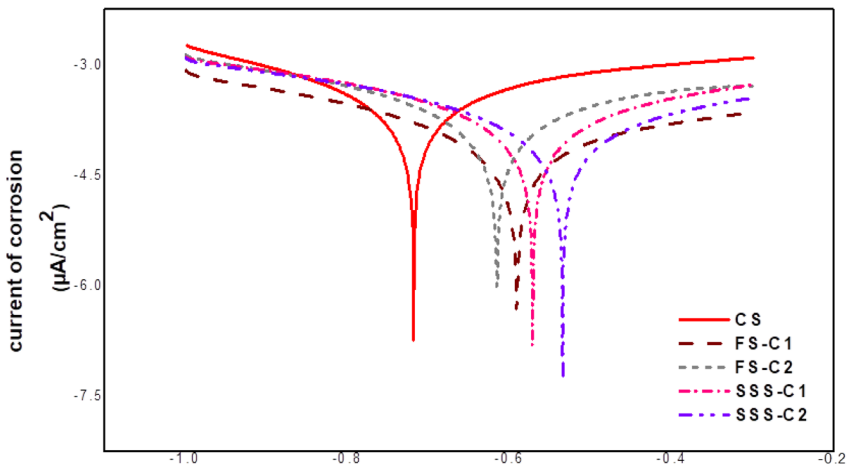


(C)

**Fig. 7** The polarization curves for several different processes before acceleration are as follows: **a** freshwater, **b** seawater, and **c** a saline solution with a 5% concentration of sodium chloride (NaCl)

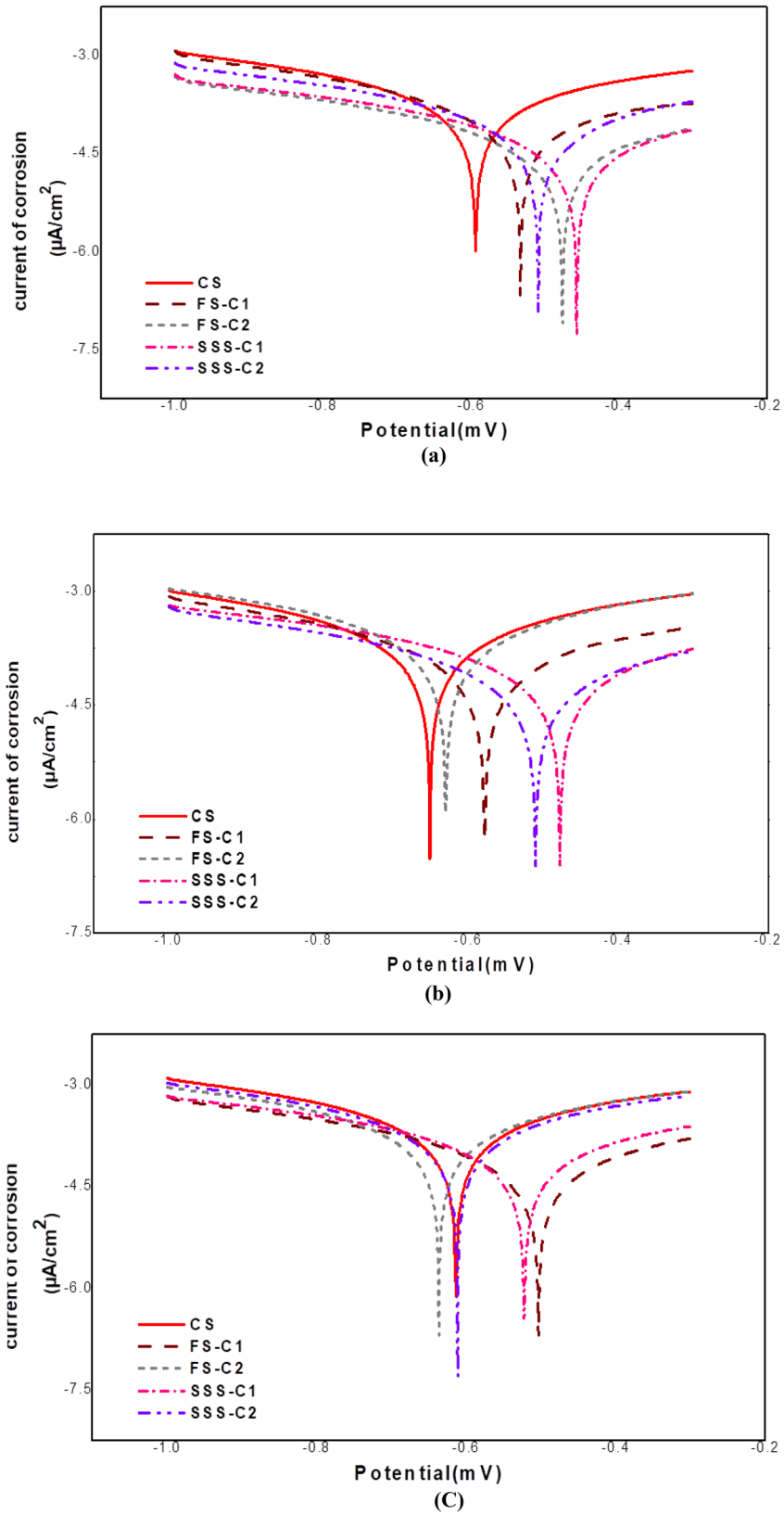


**Fig. 8** The polarization curves for several different processes after acceleration are as follows: **a** freshwater, **b** seawater, and **c** a saline solution with a 5% concentration of sodium chloride (NaCl)

**Table 12** The corrosion investigation data for freshwater, seawater, and saline solution cured series after acceleration (1 mA/cm$^2$)

| Mixture | a) Freshwater treatment series | | | | b) Seawater treatment series | | | | c) Saline solution treatment series | | | |
|---|---|---|---|---|---|---|---|---|---|---|---|---|
| | $E_{corr}$ (mV) | $R_p$ (Ω.cm$^2$) | $I_{corr}$ (μA/cm$^2$) | Corrosion rate (mm/year) | $E_{corr}$ (mV) | $R_p$ (Ω.cm$^2$) | $I_{corr}$ (μA/cm$^2$) | Corrosion rate (mm/year) | $E_{corr}$ (mV) | $R_p$ (Ω.cm$^2$) | $I_{corr}$ (μA/cm$^2$) | Corrosion rate (mm/year) |
| CS | −597.50 | 619.78 | 37.12 | 430.80 | −659.70 | 234.62 | 112.51 | 1306 | −718.60 | 223.87 | 117.70 | 1367 |
| FS-C1 | −537.90 | 1350 | 20.07 | 233.00 | −494.10 | 556.49 | 48.68 | 565.00 | −605.10 | 407.03 | 62.53 | 725.80 |
| FS-C2 | −434.60 | 923.36 | 31.05 | 360.40 | −533.00 | 584.27 | 44.01 | 510.70 | −594.20 | 428.01 | 62.69 | 727.70 |
| SSS-C1 | −449.00 | 1830 | 16.02 | 185.90 | −548.20 | 493.02 | 53.77 | 624.00 | −597.10 | 427.65 | 62.53 | 725.80 |
| SSS-C2 | −467.30 | 1710 | 16.70 | 194.10 | −410.80 | 1840 | 14.49 | 168.20 | −603.30 | 593.83 | 43.76 | 507.90 |

concrete, making them a potentially useful addition for chloride-sensitive applications (Win et al., 2004).

### 4.4 *Corrosion Rate Study Performed After Applying an Acceleration (1 mA/cm$^2$)*

This study used an expedited corrosion method to explore the long-term impacts of organisms in concrete. The CS combination treated with fresh water had a significantly greater corrosion rate than the unaccelerated mixture. This was concluded from the findings. Fig. 8a–c shows polarization curves for freshwater, seawater, and saline water at 5% sodium chloride concentration. The curves show control and treatment after being accelerated. These curves were established using an acceleration approach.

The LPR test produced separate parameter values, as shown in Table 12. *Synechocystis* sp. pcc6803 in the treated freshwater samples dramatically reduced the corrosion rate, which dropped from 430.80 mm/year to 185.90 mm/year. Similarly, *Fragilaria* sp. *CCAP1029* showed a decrease in corrosion rate of 233.00 mm/year, regardless of concentration. The reduced corrosion rate is attributed to these microbes' ability to gradually proliferate, expand, and occupy any vacant places in the mixture, successfully protecting the iron from corrosion (Wu et al., 2021; Xu et al., 2023). Surprisingly, a speedier approach resulted in zero cracks in both the control and microbe-treated groups. Furthermore, combinations exposed to seawater exhibited much higher corrosion rates than those treated with fresh water. A 5% saline solution of sodium chloride was used to speed up the corrosion process. In all treatment situations, the microalgal concrete outperformed the control concrete regarding corrosion resistance.

### 4.5 Assessment of the Effectiveness of Self-Healing Efficiency

This study looks into the process of recovering the ability of self-healing concrete to prevent water leakage and cure cracks using algal agents. After a 28-day treatment period, the specimens were purposely fractured, resulting in fissures of varied lengths. After additional 28 days of therapy, the cracks were assessed. The beams were applied in two ways: initially inside during the casting process and then externally in water. Both freshwater and seawater were used in the treatment. Algal cells were quantified using a hemocytometer or counting chamber. The results showed that the surviving algal cells accounted for nearly 85% of the initial cell count, which equated to approximately 85,000 algal cells after 28 days. This value is significant in concrete because it increases the effectiveness of crack healing.

#### *4.5.1 Internal Algal Application*

Fig. 9 shows that the control combination, which was not infected with microorganisms and was exposed to both fresh and sea water, did not improve the fractures. The research showed that algal concrete has excellent and faster-healing properties. Regardless of the concentration, the algal strain *Synechocystis* (sp. *pcc6803*) demonstrated significant and rapid crack-mending ability. The cracks in this particular sample were effectively healed in 14 days when submerged in freshwater and 7 days when immersed in seawater. This finding was reached by adding algal isolates to the mixture, which accelerated microbial-induced calcium carbonate precipitation and is corroborated by Natsi et al.'s research (Natsi & Koutsoukos, 2022). Seawater-treated microalgal concrete had a faster fracture healing rate and was more efficient than freshwater-treated concrete.

#### *4.5.2 External Algal Application*

Fig. 10 shows camera photographs of the extent of crack healing in beams after immersion in a water combination, including algae. The findings demonstrated the efficacy of applying the medication externally, with complete healing occurring between 6 to 11 days. The white curative substance retrieved from the fissures was removed from the concrete for further investigation.

### 4.6 SEM and EDX Mapping Examination Results

SEM micrographs were taken of each specimen utilized in the strength tests, which were cured in freshwater (Fig. 11) and seawater (Fig. 12). The emergence of calcite crystals is attributed to algal activity, specifically the creation of calcium carbonate. Scanning electron microscopy (SEM) images show that the specimens' inner structure produces calcite. The CS material treated in fresh and seawater had an amorphous (non-crystalline) structure. After being cured in fresh water containing $10^5$ cells/ml of *Fragilaria* (sp.*CCAP1029*), the FS-C1 specimens demonstrated a well-developed, crystalline, and homogeneous microstructure.

Furthermore, there was a significant rise in the formation of calcite crystals, as seen in Fig. 11. The SSS-C1 specimens showed substantial calcite crystal development along with a well-defined and homogeneous microstructure. *Synechocystis* (sp.*pcc6803*) cells were produced at $10^3$ cells per milliliter. Osman et al. (2024) found that the crystals had rhombohedral, spherical, and cubic forms. Densification enhanced mechanical properties while reducing corrosion. The presence of algal cells caused increased calcite precipitation via urea hydrolysis (Farid et al., 2024) and accelerated carbonation (Yang et al., 2024). Microbes have

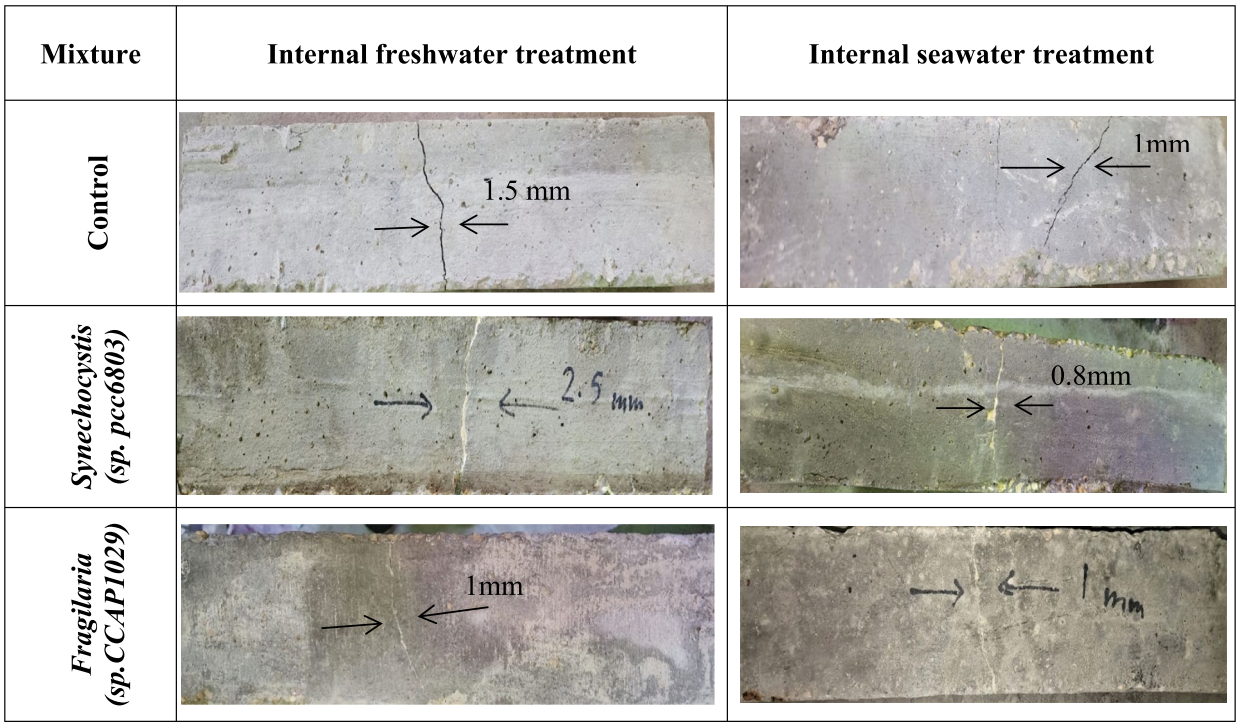


**Fig. 9** Photos illustrating the crack healing process in microbiological concrete by internal treatment

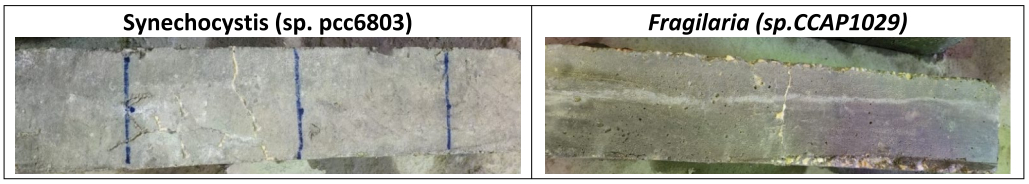


**Fig. 10** Photos illustrating the crack healing process in microbiological concrete by external treatment

significantly improved concrete's self-healing, durability, and mechanical strength.

When treated to seawater curing, the CS matrix (Fig. 12) developed a disordered and mushy texture, most likely due to the negative impacts of seawater. The FS-C1 matrix has a greater rate of calcite crystalline growth than the SSS-C1. Algae have a unique ability to grow in the presence of seawater, and they can precipitate larger amounts of calcite. The scanning electron microscopy (SEM) study revealed well-defined calcite crystals embedded in the concrete matrix. The higher calcium levels discovered point to the presence of calcite, specifically calcium carbonate. Fig. 12 [location 3 (2 μm)] shows the coexistence of algae organisms with crystalline calcium carbonate, demonstrating their significance in calcite precipitation as a protective barrier against hazardous chemicals.

A mapping investigation utilizing EDX was performed on the concrete samples to provide additional evidence of calcite development. Fig. 13 shows mapping pictures of freshwater-cured mixes (CS, SSS-C1, and FS-C1) and seawater-cured mixes (CS, SSS-C1, and FS-C1). Table 13 shows the findings of the EDX study performed on the freshwater treatment series. It demonstrates that oxygen, calcium, and carbon atoms are the most common components found in all groups. The carbon concentration in the freshwater-cured CS specimen was 10.67%. This figure rose to 24.04% in SSS-C1 and 23.13% in FS-C1. The increase in calcium and carbon levels can be attributed to bacteria, which explains the previously mentioned improvement in concrete qualities. Table 13 shows the seawater treatment series's chemical elements, as EDX discovered in Fig. 14. All groups have been validated to contain the required elements. The calcium content of the CS specimen treated in saltwater was 2.3%. This

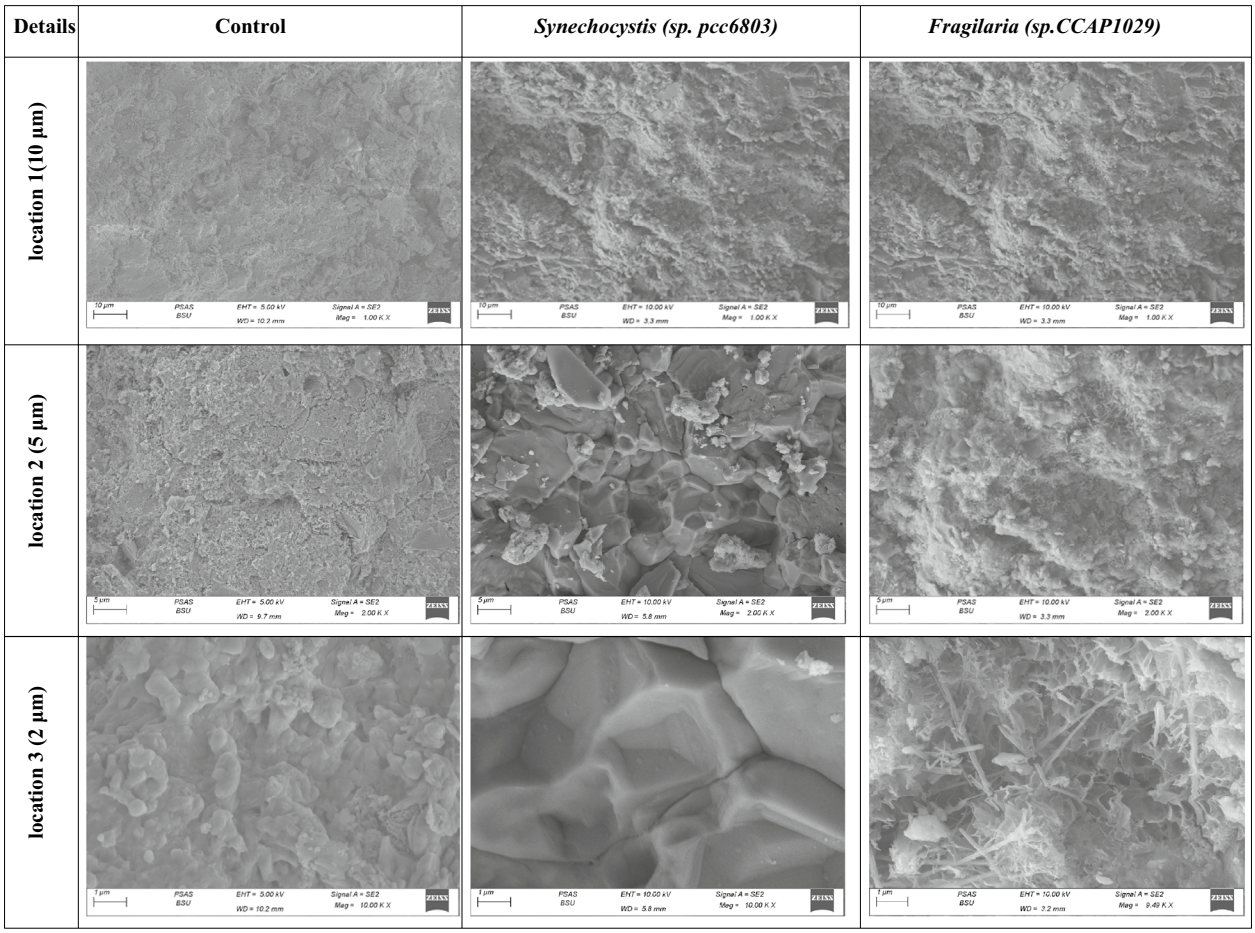


**Fig. 11** Details at various locations of the SEM photographs of algal specimens cured fresh water

percentage increased to 17.23% for SSS-C1 and 13.94% for FS-C1. The algae showed a strong sensitivity to the seawater treatment. Compared to freshwater treatment, seawater application resulted in a much higher percentage of treated calcium.

## 5 Conclusions and Recommendations

The results of the above-mentioned inquiries suggest the following conclusions:

- Microalgae and cyanobacteria can improve mechanical properties and heal cracks in concrete.
- Almost all microalgal specimens showed increased mechanical properties after 7 and 28 days of seawater curing compared to fresh water-cured concrete. However, after 90 days, their mechanical properties deteriorated compared to those treated in fresh water.
- This discovery can be explained by the fact that algae cells had a higher survival rate in seawater during previous eras. The substance's availability in seawater declines over time but increases in freshwater conditions.
- The FS-C1 and SSS-C1 algae series, containing $10^3$ cells/ml of *Fragilaria* sp.*CCAP1029* and *Synechocystis* sp.*pcc6803*, respectively, improved the mechanical properties of concrete in freshwater settings.
- The SSS-C1 series outperformed the CS series by 21.46%, 18.12%, and 21.66% on the 7th, 28th, and 90th days of curing in fresh water. The splitting tensile strengths of the SSS-C1 series rose by 1.2%, 3.23%, and 16.67% compared to the CS series. These values exceeded those observed in the CS series.
- FS-C1 cells immersed in seawater for 7, 28, and 90 days showed increased compressive and tensile strength. When cured in seawater, the FS-C1 series had 11.82%, 15.97%, and 9.86% higher 7th, 28th, and 90th compressive strengths than the CS series. The FS-C1 series increased 7th splitting tensile strength by 4.00%, 28th by 9.68%, and 90th by 16.77%. Seawater enhanced FS-C1 and FS-C2 compressive and splitting strengths on the 7th, 28th, and 90th days.

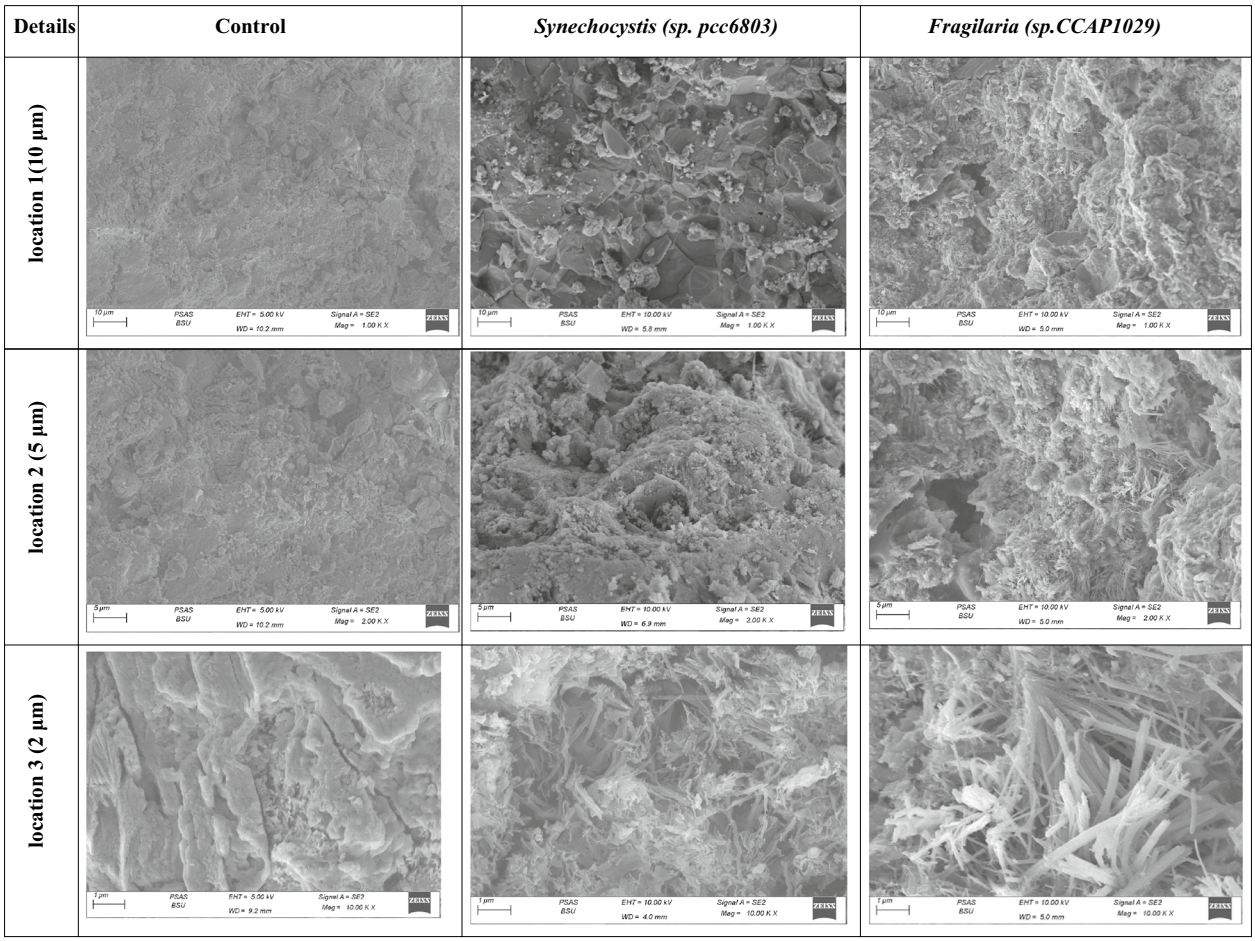


**Fig. 12** Details at various locations of the SEM micrographs of algal specimens cured seawater

- Before accelerating the process with fresh water, it was observed that increasing the concentration of any of the microbes in the cells was associated with a lower maximum anodic current and improved passive layer quality. Research has demonstrated that algal species have a significant impact on the durability of reinforcing steel in concrete. The microbiological precipitation of minerals produced by the algae helps maintain the passive layer of reinforcing steel and prevents corrosion.
- The research implements the accelerated corrosion technique to examine the long-term impacts of microbial application on concrete. The fresh-water cured CS mixture exhibited elevated quantities of calcite deposits. After acceleration, After acceleration, it saw a significant decrease in corrosion rate compared to the non-accelerated mix.
- Algal pigments, namely β-carotene pigment, contribute to increased strength.
- Carotene pigment is a hydrocarbon compound that follows the conjugated diene system. This approach causes a significant concentration of electrons within the concrete structure, filling the pores and reducing permeability while increasing compressive strength.
- The alga produces calcite as a byproduct of photosynthesis. The findings will show that including algae cells can increase the compressive strength of concrete.

Based on the inferred findings, the following suggestions are proposed:

- Research should focus on the role of various algae species.

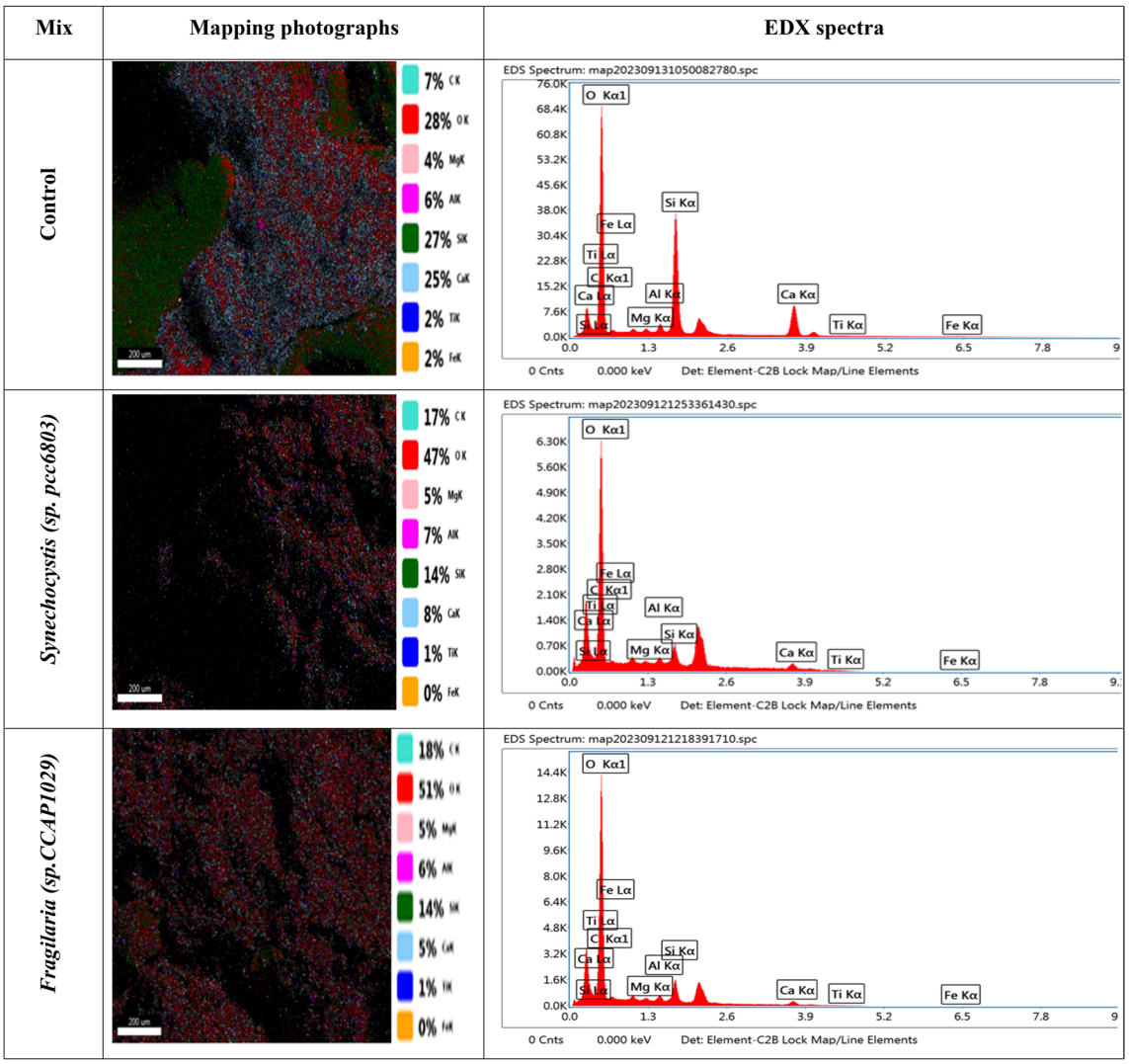


**Fig. 13** Mapping photographs and EDX spectra of freshwater treatment

**Table 13** The chemical elements of fresh and seawater treatment series by EDX

| Element | a) Freshwater treatment | | | | | | b) Seawater treatment | | | | | |
|---|---|---|---|---|---|---|---|---|---|---|---|---|
| | CS | | SSS-C2 | | FS-C2 | | CS | | SSS-C2 | | FS-C2 | |
| | Weight% | Atoms% | Weight% | Atoms% | Weight% | Atoms% | Weight% | Atoms% | Weight% | Atoms% | Weight% | Atoms% |
| C | 10.67 | 15.70 | 24.04 | 30.98 | 23.13 | 29.69 | 17.87 | 26.62 | 17.52 | 24.81 | 11.38 | 16.77 |
| O | 62.65 | 69.20 | 66.62 | 64.45 | 68.39 | 65.93 | 71.16 | 69.11 | 62.08 | 66.00 | 63.13 | 69.83 |
| Mg | 0.82 | 0.59 | 0.87 | 0.55 | 1.12 | 0.71 | 1.4 | 0.48 | 0.51 | 0.36 | 0.85 | 0.62 |
| Al | 1.36 | 0.89 | 1.39 | 0.79 | 1.28 | 0.73 | 1.75 | 0.52 | 0.51 | 0.32 | 1.78 | 1.17 |
| Si | 15.13 | 9.52 | 3.35 | 1.85 | 3.87 | 2.13 | 4.52 | 2.60 | 1.79 | 1.09 | 8.41 | 5.30 |
| Ca | 9.05 | 3.99 | 2.72 | 1.05 | 1.64 | 0.63 | 2.3 | 0.52 | 17.23 | 7.31 | 13.94 | 6.16 |
| Ti | 0.09 | 0.03 | 1.01 | 0.33 | 0.58 | 0.19 | 0.99 | 0.16 | 0.11 | 0.04 | 0.12 | 0.04 |
| Fe | 0.23 | 0.07 | 0.09 | 0.03 | 0.01 | 0.02 | 0.28 | 0.10 | 0.26 | 0.08 | 0.39 | 0.12 |

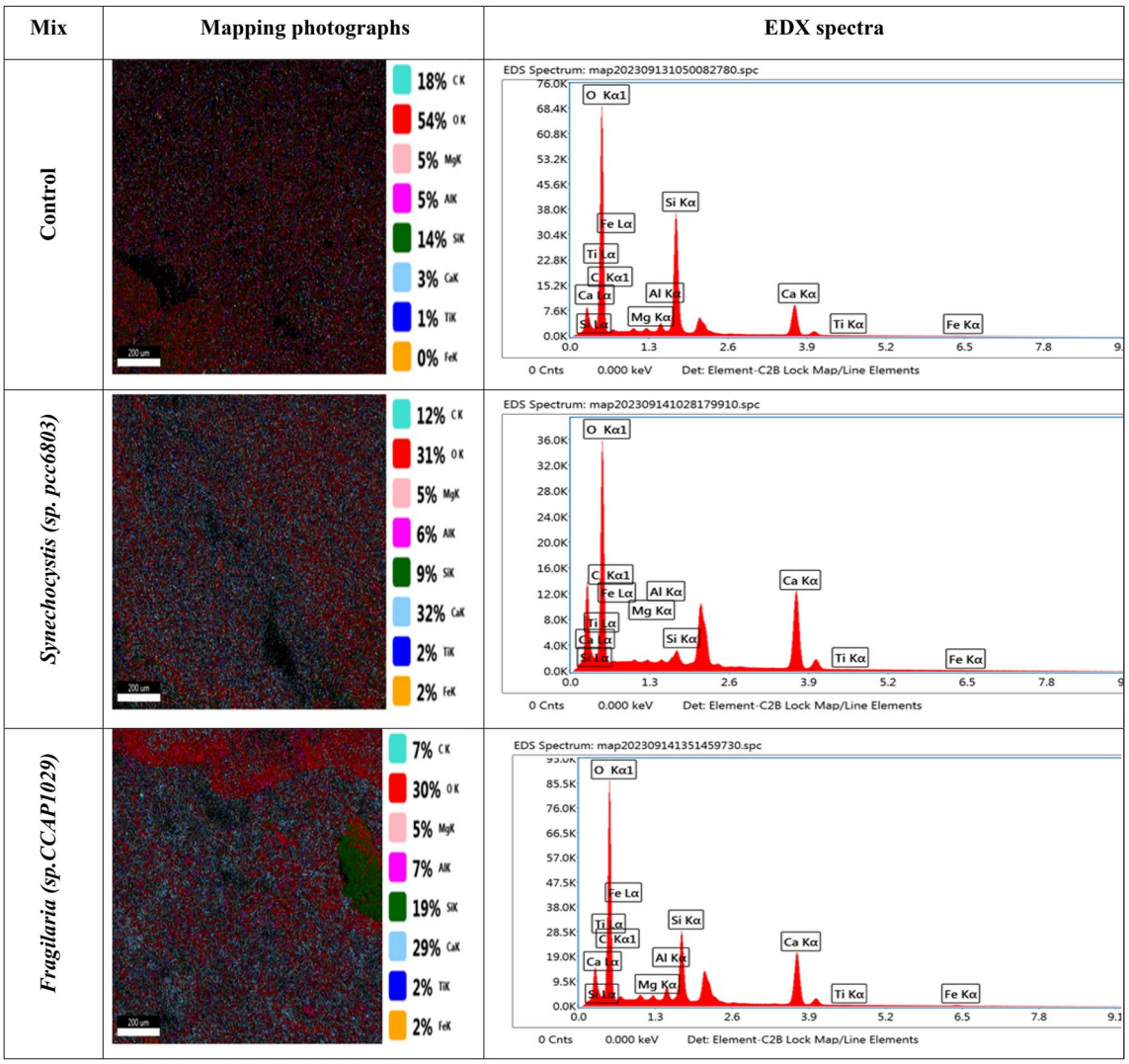


**Fig. 14** Mapping photographs and EDX spectra of seawater treatment

- Maximize the benefits of concrete additives by including or immobilizing bacteria, fungi, and algae.
- Mixing different types of algae.
- Longer-term evaluation (e.g., 180 days or 1 year).

**Acknowledgements**
Not applicable.

**Author contributions**
A. Serag Farid: Conceptualization, methodology, supervision, review. Shireen T. M. Yousef: Investigation, data curation, writing—original draft. Mohamed M. Abdelaziz: Methodology, supervision, review. G. M. Abd-El Hafez: Data curation,review. Ali A. E. El-Khateb: Conceptualization, methodology, supervision, review. Khaled N. M. Elsayed: Conceptualization, methodology, review. All authors read and approved the final manuscript.

**Funding**
Open access funding provided by The Science, Technology & Innovation Funding Authority (STDF) in cooperation with The Egyptian Knowledge Bank (EKB). This research received no specific grant from funding agencies in the public, commercial, or not-for-profit sectors.

**Availability of data and materials**
The datasets used and/or analysed during the current study are available from the corresponding author on reasonable request.

## Declarations

**Ethics approval and consent to participate**
Not applicable.

**Consent for publication**
Not applicable.

**Competing interests**
The authors declare that they have no competing interests.

Received: 31 July 2024 Accepted: 9 May 2025
Published online: 14 July 2025

**References**


Achal, V., Pan, X., & Özyurt, N. (2011). Improved strength and durability of fly ash-amended concrete by microbial calcite precipitation. *Ecological Engineering, 37*(4), 554–559. https://doi.org/10.1016/j.ecoleng.2010.11.009

Agha, W. N. (2024). A framework for assessing sustainability in post-disaster reconstruction projects on the example of Syria. *Steps for Civil, Construction and Environmental Engineering, 2*(2), 17–31.

Amran, M., et al. (2022). Self-healing concrete as a prospective construction material: A review. *Materials (Basel), 15*(9), 1–46. https://doi.org/10.3390/ma15093214

Ariyanti, D. (2012). Feasibility of using microalgae for biocement production through biocementation. *Journal of Bioprocess and Biotechnology*. https://doi.org/10.4172/2155-9821.1000111

Awad, Z. (2023). Sustainable restoration techniques for historic buildings in Tyre City. *Steps for Civil, Construction and Environmental Engineering, 1*(1), 10–17.

Banthia, N., Biparva, A., & Mindess, S. (2005). Permeability of concrete under stress. *Cement and Concrete Research, 35*(9), 1651–1655. https://doi.org/10.1016/j.cemconres.2004.10.044

Bending, G. D., et al. (2017). An overview of biocement production from microalgae. *International Journal of Science and Engineering, 9*(1), 36–40. https://doi.org/10.12777/ijse.2.2.31-33

Castanier, S., Le Métayer-Levrel, G., & Perthuisot, J. P. (1999). Ca-carbonates precipitation and limestone genesis - the microbiogeologist point of view. *Sedimentary Geology*. https://doi.org/10.1016/S0037-0738(99)00028-7

Cement, H., & Apparatus, A. (2016). *Standard specification for portland cement*. pp 1–10. https://doi.org/10.1520/C0150.

Dagade, A. S. & Thakur S. R. (2020). Use of bacillus bacteria in self-healing concrete; 2020. pp 7707–7709.

Dasar, A., Patah, D., Hamada, H., Sagawa, Y., & Yamamoto, D. (2020). Applicability of seawater as a mixing and curing agent in 4-year-old concrete. *Construction and Building Materials, 259*, Article 119692. https://doi.org/10.1016/j.conbuildmat.2020.119692

De Muynck, W., De Belie, N., & Verstraete, W. (2010). Microbial carbonate precipitation in construction materials: A review. *Ecological Engineering, 36*(2), 118–136.

Delgado, C., Novais, M. H., Blanco, S., & Almeida, S. F. P. (2015). Examination and comparison of Fragilaria candidagilae sp. Nov. with type material of *Fragilaria recapitellata*, *F. capucina*, *F. perminuta*, *F. intermedia* and *F. neointermedia* (Fragilariales, Bacillariophyceae). *Phytotaxa, 231*(1), 1–18. https://doi.org/10.11646/phytotaxa.231.1.1

Dev, U., Singh, T., Babu, T., Mandal, A. K., Sharma, M., & Mandal, A. (2025). Enhancing blood platelet counting through deep learning models for advanced diagnostics. *SN Computer Science, 6*(1), 1–10.

Dharmabiksham, B., Kavya, C., & Kapilan, S. (2023). The experimental performance of durability and strength to repair for micro cracks in a self-healing bacterial concrete. *Materials Today: Proceedings*. https://doi.org/10.1016/j.matpr.2023.04.328

Dharmabiksham, B., & Murali, K. (2022). Experimental investigation on the strength and durability aspect of bacterial self-healing concrete with GGBS and dolomite powder. *Materials Today: Proceedings, 66*, 1156–1161. https://doi.org/10.1016/j.matpr.2022.04.955

Dianti, Y. (2017). Cyanobacteria,periphyton and aquatic macrophytes. *Angewandte Chemie International.* 6(11): 951–952, pp 5–24.

Elsayed, K. N. M., Mohamed, A. M., Noke, A., & Klöck, G. (2017). Microalgae as an alternative source for biodiesel and biogas production—a mini review. *Вестник Росздравнадзора, 4*(1), 9–15. https://doi.org/10.7537/marnsj151217.01.Key

Farid, A. S., Yousef, S. T. M., Abd-El Hafez, G. H. M., Elsayed, K. N. M., El-Khateb, A. A. E., & Abdelaziz, M. M. (2024). Effect of novel gram-positive bacteria and fungi on the durability, corrosion resistance performance, and self-healing ability of concrete over various curing conditions. *Journal of Sustainable Cement-Based Materials*. https://doi.org/10.1080/21650373.2024.2338555

Fratzl, P. (2014). Self-healing materials: An alternative approach to 20 centuries of materials science. *Chemistry International Newsmagazine for IUPAC, 30*(6), 20–21. https://doi.org/10.1515/ci.2008.30.6.20

Garg, R., Garg, R., & Eddy, N. O. (2023). Microbial induced calcite precipitation for self-healing of concrete: A review. *Journal of Sustainable Cement-Based Materials, 12*(3), 317–330. https://doi.org/10.1080/21650373.2022.2054477

Gonen, T., & Yazicioglu, S. (2007). The influence of compaction pores on sorptivity and carbonation of concrete. *Construction and Building Materials., 21*, 1040–1045. https://doi.org/10.1016/j.conbuildmat.2006.02.010

Gupta, S. G., Rathi, C., & Kapur, S. (2013). Biologically Induced Self Healing Concrete: A Futuristic Solution for Crack Repair. *International Journal of Applied Science and Biotechnology, 1*(3), 85–89. https://doi.org/10.3126/ijasbt.v1i3.8582

Hammes, F., & Verstraete, W. (2002). *Key roles of pH and calcium metabolism in microbial carbonate precipitation*. Morito 1980. pp 3–7.

Huseien, G. F., Mirza, J., Ariffin, N. F., & Hussin, M. W. (2015). Synthesis and characterization of shelf-healing mortar with modified strength. *Jurnal Teknologi, 76*(1), 195–200. https://doi.org/10.11113/jt.v76.3688

I. Units, *An ACI Standard*. .

IS 516. (1959). *Method of tests for strength of concrete*. Bur. Indian Stand. pp 1–30.

Jadhav, A. G., & Deore, K. M. (2022). A review on self healing concrete by using bacillus megaterium. *International Research Journal of Engineering and Technology, 9*, 1682–1689.

Jahami, A., Younes, H., & Khatib, J. (2023). Enhancing reinforced concrete beams: Investigating steel dust as a cement substitute. *Infrastructures, 8*(11), 157.

Jahami, A., Zeaiter, N., & Cheaib, M. (2024). Reviewing the potential: A comprehensive review of natural fibers (NFs) in structural concrete and their multifaceted influences. *Innovative Infrastructure Solutions, 9*(4), 102.

Jongvivatsakul, P., Janprasit, K., Nuaklong, P., Pungrasmi, W., & Likitlersuang, S. (2019). Investigation of the crack healing performance in mortar using microbially induced calcium carbonate precipitation (MICP) method. *Construction and Building Materials, 212*, 737–744. https://doi.org/10.1016/j.conbuildmat.2019.04.035

Jonkers, H. M., & Schlangen, E. (2008). Development of a bacteria-based self healing concrete. *Tailor Made Concrete Structures, 1*, 425–430.

Jonkers, H. M., Thijssen, A., Muyzer, G., Copuroglu, O., & Schlangen, E. (2010). Application of bacteria as self-healing agent for the development of sustainable concrete. *Ecological Engineering, 36*(2), 230–235. https://doi.org/10.1016/j.ecoleng.2008.12.036

Joseph, A., Aikawa, S., Sasaki, K., Matsuda, F., Hasunuma, T., & Kondo, A. (2014). Increased biomass production and glycogen accumulation in apcE gene deleted Synechocystis sp. PCC 6803. *AMB Express, 4*, 1–6.

Kanwal, M., Khushnood, R. A., Adnan, F., Wattoo, A. G., & Jalil, A. (2023). Assessment of the MICP potential and corrosion inhibition of steel bars by biofilm forming bacteria in corrosive environment. *Cement and Concrete Composites, 137*, Article 104937. https://doi.org/10.1016/j.cemconcomp.2023.104937

Kaushal, V., & Saeed, E. (2024). *Sustainable and innovative self-healing concrete technologies to mitigate environmental impacts in construction sustainable and innovative self-healing concrete construction*. https://doi.org/10.20944/preprints202405.0655.v1.

Khanafari, A., Khams, F. N., & Sepahy, A. A. (2011). An investigation of biocement production from hard water. *Middle-East Journal of Scientific Research, 7*(6), 964–971.

Lachimpadi, S. K., Pereira, J. J., Taha, M. R., & Mokhtar, M. (2012). Construction waste minimisation comparing conventional and precast construction (Mixed System and IBS) methods in high-rise buildings: A Malaysia case study. *Resources, Conservation and Recycling, 68*, 96–103. https://doi.org/10.1016/j.resconrec.2012.08.011

Lam, T. Q. K., Sreekeshava, K. S., Bhargavi, C., Ganesh, C. R., Ambale, N. S., & Do, T. M. D. (2024). Exploring the potential of green microalgae-based phycoremediation treated wastewater for sustainable concrete production. *Advances in Civil Engineering*. https://doi.org/10.1155/2024/8564202

Li, P., Li, W., Sun, Z., Shen, L., & Sheng, D. (2021). Development of sustainable concrete incorporating seawater: A critical review on cement hydration, microstructure and mechanical strength. *Cement and Concrete Composites, 121*, Article 104100. https://doi.org/10.1016/j.cemconcomp.2021.104100

Li, X., Li, D., & Xu, Y. (2019). Modeling the effects of microcracks on water permeability of concrete using 3D discrete crack network. *Composite Structures, 210*, 262–273. https://doi.org/10.1016/j.compstruct.2018.11.034

Linda, R., Prabowo, H., & Indrayadi, I. (1832). Review on the potential application of bacterial cementitious composites in Indonesia. *Journal of Physics: Conference Series, 1*, 2021. https://doi.org/10.1088/1742-6596/1832/1/012004

Method, F. T. (2018). iTeh standards iTeh standards document preview. I(7916): 1–3. https://doi.org/10.1520/D1193-06R18.1.
Mohamed, M. H. H., et al. (2022). Flocculation of microalgae using calcium oxide nanoparticles; process optimization and characterization. *International Aquatic Research, 14*(1), 63–70. https://doi.org/10.22034/IAR.2022.1943339.1206
Natsi, P. D., & Koutsoukos, P. G. (2022). Calcium carbonate mineralization of microalgae. *Biomimetics, 7*(4), 1–19. https://doi.org/10.3390/biomimetics7040140
Neville, A. M., & Brooks, J. J. (1987). *Concrete Technology*. Longman Scientific & Technical England.
Niveditha, C., Sarayu, K., Ramachandra Murthy, A., Ramesh Kumar, V., & Iyer, N. R. (2018). Marine algae for cement mortar strengthening. *Journal of Civil Engineering Research, 2014*(2A), 23–25. https://doi.org/10.5923/c.jce.201401.05
Nur, M. M. A., & Dewi, R. N. (2024). Opportunities and challenges of microalgae in biocement production and self-repair mechanisms. *Biocatalysis and Agricultural Biotechnology, 56*, Article 103048. https://doi.org/10.1016/j.bcab.2024.103048
Olivia, M., Moheimani, N., Javaherdashti, R., Nikraz, H. R., & Borowitzka, M. A. (2013). The influence of micro algae on corrosion of steel in fly ash geopolymer concrete: A preliminary study. *Advances in Materials Research, 626*, 861–866. https://doi.org/10.4028/www.scientific.net/AMR.626.861
Osman, A. I., et al. (2024). *Synthesis of green nanoparticles for energy, biomedical, environmental, agricultural, and food applications: A review* (2nd ed., Vol. 22). Springer International Publishing.
Osman, K. M., Taher, F. M., Abd El-Tawab, A., & Faried, A. S. (2021). Role of different microorganisms on the mechanical characteristics, self-healing efficiency, and corrosion protection of concrete under different curing conditions. *Journal of Building Engineering, 41*, Article 102414. https://doi.org/10.1016/j.jobe.2021.102414
Picandet, V., Khelidj, A., & Bellegou, H. (2009). Crack effects on gas and water permeability of concretes. *Cement and Concrete Research, 39*(6), 537–547. https://doi.org/10.1016/j.cemconres.2009.03.009
Rais, M. S., & Khan, R. A. (2021). Experimental investigation on the strength and durability properties of bacterial self-healing recycled aggregate concrete with mineral admixtures. *Construction and Building Materials, 306*, Article 124901. https://doi.org/10.1016/j.conbuildmat.2021.124901
Ramachandran, S. K., Ramakrishnan, V., & Bang, S. S. (2001). Remediation of concrete using microorganisms. *Material Journal, 98*(1), 3–9.
S. Recommendation (2016). *Guidance on the use of I. S. EN 12620 : 2002 + A1: 2008—aggregates for concrete*.
Seifan, M., Sarmah, A. K., Samani, A. K., Ebrahiminezhad, A., Ghasemi, Y., & Berenjian, A. (2018). Mechanical properties of bio self-healing concrete containing immobilized bacteria with iron oxide nanoparticles. *Applied Microbiology and Biotechnology, 102*, 4489–4498.
Sikora, P., Cendrowski, K., Abd, M., & Chung, S. Y. (2020). The effects of seawater on the hydration, microstructure and strength development of Portland cement pastes incorporating colloidal silica. *Applied Nanoscience, 10*(8), 2627–2638. https://doi.org/10.1007/s13204-019-00993-8
Stehlík, M., Heřmánková, V., & Vítek, L. (2015). Opening of microcracks and air permeability in concrete. *Journal of Civil Engineering and Management, 21*(2), 177–184. https://doi.org/10.3846/13923730.2013.802721
Taher, F. M., Faried, A. S., El-Tawab, A. A., & Osman, K. M. (2020). Effect of dunaliella salina alga on compressive strength of concrete. *International Research Journal of Engineering and Technology, 7*, 1675–1679.
Van Tittelboom, K., De Belie, N., De Muynck, W., & Verstraete, W. (2010). Use of bacteria to repair cracks in concrete. *Cement and Concrete Research, 40*(1), 157–166. https://doi.org/10.1016/j.cemconres.2009.08.025
Verma, P., & Kaur, J. (2020). Diatoms analysis of well water sample of different districts of Punjab region. *International Journal of Forensic Sciences, 5*(3), Article 000202.
Wang, J., et al. (2022). Effect of phaeodactylum tricornutum in seawater on the hydration of blended cement pastes. *Coatings, 12*(11), 1639.
Whiffin, V. S. (2004). *Microbial $CaCO_3$ precipitation for the production of biocement*. Perth: Murdoch University. Thesis, pp 20.
Wiktor, V., & Jonkers, H. M. (2011). Quantification of crack-healing in novel bacteria-based self-healing concrete. *Cement and Concrete Composites, 33*(7), 763–770.
Wiktor, V., & Jonkers, H. M. (2016). Bacteria-based concrete: From concept to market. *Smart Materials and Structures, 25*(8), Article 084006. https://doi.org/10.1088/0964-1726/25/8/084006
Win, P. P., Watanabe, M., & Machida, A. (2004). Penetration profile of chloride ion in cracked reinforced concrete. *Cement and Concrete Research, 34*(7), 1073–1079. https://doi.org/10.1016/j.cemconres.2003.11.020
Wu, X., Luo, Y., Yang, W., Gao, Y., Bi, Y., & Xie, Y. (2021). Effect of rehydration of unhydrated cement on ultra-high performance concrete after heat curing. *Ceramics-Silikaty, 65*(3), 305–315. https://doi.org/10.13168/cs.2021.0032
Xu, Z., Zhang, T., Wan, H., Liu, H., Gu, T., & Liu, H. (2023). Accelerated development of Ti-6Al-4V microbial corrosion triggered by electroactive sulfate-reducing Desulfovibrio ferrophilus biofilm in enriched artificial seawater containing soluble electron shuttle. *Corrosion Science, 220*, Article 111306. https://doi.org/10.1016/j.corsci.2023.111306
Yang, Y., Tang, S., & Chen, J. P. (2024). Carbon capture and utilization by algae with high concentration CO2 or bicarbonate as carbon source. *Science Total Environment, 918*, Article 170325. https://doi.org/10.1016/j.scitotenv.2024.170325
Yang, Z., Hollar, J., He, X., & Shi, X. (2011). A self-healing cementitious composite using oil core/silica gel shell microcapsules. *Cement and Concrete Composites, 33*(4), 506–512. https://doi.org/10.1016/j.cemconcomp.2011.01.010
Yatish Reddy, P. V., Ramesh, B., & Prem Kumar, L. (2020). Influence of bacteria in self healing of concrete - a review. *Materials Today Proceedings, 33*, 4212–4218. https://doi.org/10.1016/j.matpr.2020.07.233
Yuvaraj, S., Nirmalkumar, K., Kumar, V. R., Gayathri, R., Mukilan, K., & Shubikksha, S. (2022). Influence of corrosion inhibitors in reinforced concrete—a state of art of review. *Materials Today: Proceedings, 68*, 2406–2412. https://doi.org/10.1016/j.matpr.2022.09.118
Zeaiter, H., Jahami, A., & Khatib, J. (2023). Bio-concrete and beyond: Advancements in self-healing techniques for durable infrastructure. *Step for Civil, Construction and Environmental Engineering, 1*(1), 18–29.
Zhang, L. V., et al. (2021). Crack self-healing in bio-green concrete. *Composites Part B: Engineering., 227*, Article 109397. https://doi.org/10.1016/j.compositesb.2021.109397

## Publisher's Note



**A. Serag Farid** Professor at the Faculty of Engineering, Fayoum University, Egypt.

**Shireen T. M. Yousef** Master Student at the Faculty of Engineering, Fayoum University, Egypt.

**Mohamed M. Abdelaziz** Assistant professor at the Faculty of Engineering, Fayoum University, Egypt.

**G. M. Abd-El Hafez** Assistant Professor at the Faculty of Science, Fayoum University, Egypt.

**Ali A. E. El-Khateb** Professor at the Faculty of Engineering, Assiut University, Egypt.

**Khaled N. M. Elsayed** Associate Professor at the Faculty of Science, Beni-Suef University, Egypt.